

Petrography and geochemistry of the late Eocene–early Oligocene submarine fans and shelf deposits on Lemnos Island, NE Greece. Implications for provenance and tectonic setting

A. MARAVELIS and A. ZELILIDIS*

Department of Geology, University of Patras, Greece

Provenance and tectonic history of the late Eocene–early Oligocene submarine fans and shelf deposits on Lemnos Island, NE Greece, were studied using sandstone framework composition, sedimentological data and sandstone and mudstone geochemistry. The resulting tectonic–sedimentological model is based on the late Eocene–early Oligocene Lemnos Island being in a forearc basin with the outer arc ridge as a major sediment source. Modal petrographic analysis of the studied sandstones shows that the source area comprises sedimentary, metamorphic and plutonic igneous rocks deposited in the studied area in a recycled orogenic environment. Moreover, within the above sediments, the minor occurrence of volcanic fragments suggests little or no influence of a volcanic source. Provenance results, based on major, trace and rare earth element (REE) data, suggest an active continental margin/continental island arc signature. All the samples are LREE, enriched relative to HREE, with a flat HREE pattern and positive Eu anomalies, suggesting that the processes of intracrustal differentiation (involving plagioclase fractionation) were not of great importance. Results derived from the multi-element diagrams also suggest an active margin character, and a mafic/ultramafic source rock composition, while the positive anomaly of Zr that can be attributed to a passive continental margin source, is most likely associated with reworking and sorting during sediment transfer. Palaeocurrents, with a NE–NNE direction, indicate a northeast flow, towards the location of the late Eocene–early Oligocene magmatic belt in the north-east Aegean region. Conglomerates are composed of chert, gneiss and igneous fragments, such as basalts and gabbros, suggesting this outer arc ridge as a likely source area. Copyright © 2009 John Wiley & Sons, Ltd.

Received 20 February 2009; accepted 13 August 2009

KEY WORDS geochemistry; provenance; sandstone petrography; submarine fans; Lemnos Island; Greece

1. INTRODUCTION

The use of sedimentary petrography for provenance studies is a standard method in sedimentology and basin analysis. Discrimination fields, based on the ratio of the major clastic components, as quartz, feldspar and rock fragments, have been built from well-known tectonic and sedimentary settings, in order to interpret clastic deposits of any age, setting and location on Earth (e.g. Dickinson and Suczek 1979; Ingersoll and Suczek 1979; Dickinson 1985; Zuffa 1985). More recently, major and trace element bulk-rock analyses have been used in several studies to reconstruct the tectonic and sedimentary setting of clastic sedimentary basins (Kutterolf *et al.* 2007). Since different plate tectonic configurations produce diverse magmatic suites (Bonin

et al. 1993), of different chemical characteristics (which are transferred from the primary to the sedimentary rock) chemical patterns are used to discriminate geotectonic settings from sediments (Crook 1974; Bhatia 1983; Roser and Korsch 1988), and have been applied in recent publications (Kroonenberg 1994; Burnett and Quirk 2001; Zimmermann and Bahlburg 2003; Armstrong-Altrin *et al.* 2004; Wanas and Abdel-Maguid 2006). The geochemical analysis of sedimentary rocks (such as matrix-rich sandstones) is a valuable tool for provenance studies, as long as the bulk composition is not strongly affected by diagenesis, metamorphism or other alteration processes (McLennan *et al.* 1993). Trace elements (e.g. Ti, Nb, Ta, Cs, Ce, Ni, V, Co, Y, La, Th, Sc and Zr) are particularly useful for provenance analysis, as they are insoluble and usually immobile under surface conditions. On account of their predictable behaviour during fractional crystallization, weathering and recycling, these sediments preserve characteristics of the source rocks in the

* Correspondence to: A. Zelilidis, Department of Geology, University of Patras, Greece. E-mail: A.Zelilidis@upatras.gr

sedimentary record (Taylor and McLennan 1985; Bhatia and Crook 1986; McLennan 1989; McLennan *et al.* 1993; Roser *et al.* 1996). Therefore, trace elements represent well-established provenance and tectonic setting indicators (Bhatia and Crook 1986; McLennan 2001). Rare Earth Elements (REE) also represent well-established provenance indicators (McLennan *et al.* 1990, 1993; McLennan 2001). Although many studies have shown that REE can be mobilized during weathering and/or diagenesis (Milošowski and Zalasiewicz 1991; Zhao *et al.* 1992; Bock *et al.* 1994; McDaniel *et al.* 1994; Uetzmann *et al.* 2002) often, they are immobile under surface conditions, and therefore, the characteristics of the source rocks are preserved in the sedimentary record (Taylor and McLennan 1985). The purpose of this study is to combine original petrographic and geochemical data to the study of Palaeogene deep-sea clastic sediments, with data from stratigraphy and field

sedimentology, in order to establish their geological setting within the eastern Mediterranean Sea region.

2. GEOLOGICAL SETTING

The study area lies in NE Aegean Sea, Greece. The plate configuration of the Aegean region (Figure 1) consists of the Aegean Plate to the south separated by a strike-slip boundary (McKenzie 1970; Papazachos *et al.* 1998) from the Eurasian Plate to the north, which encompasses the north Aegean, Rhodope and adjacent areas. The Aegean Plate is overriding the African Plate, accommodated by northeastward dipping subduction in the Hellenic Trench. The strike-slip boundary between the Aegean and the Eurasian plates (the north Aegean transform zone) consists of two major strike-slip faults, which are extensions of the North Anatolian Fault. Convergence between the Eurasian

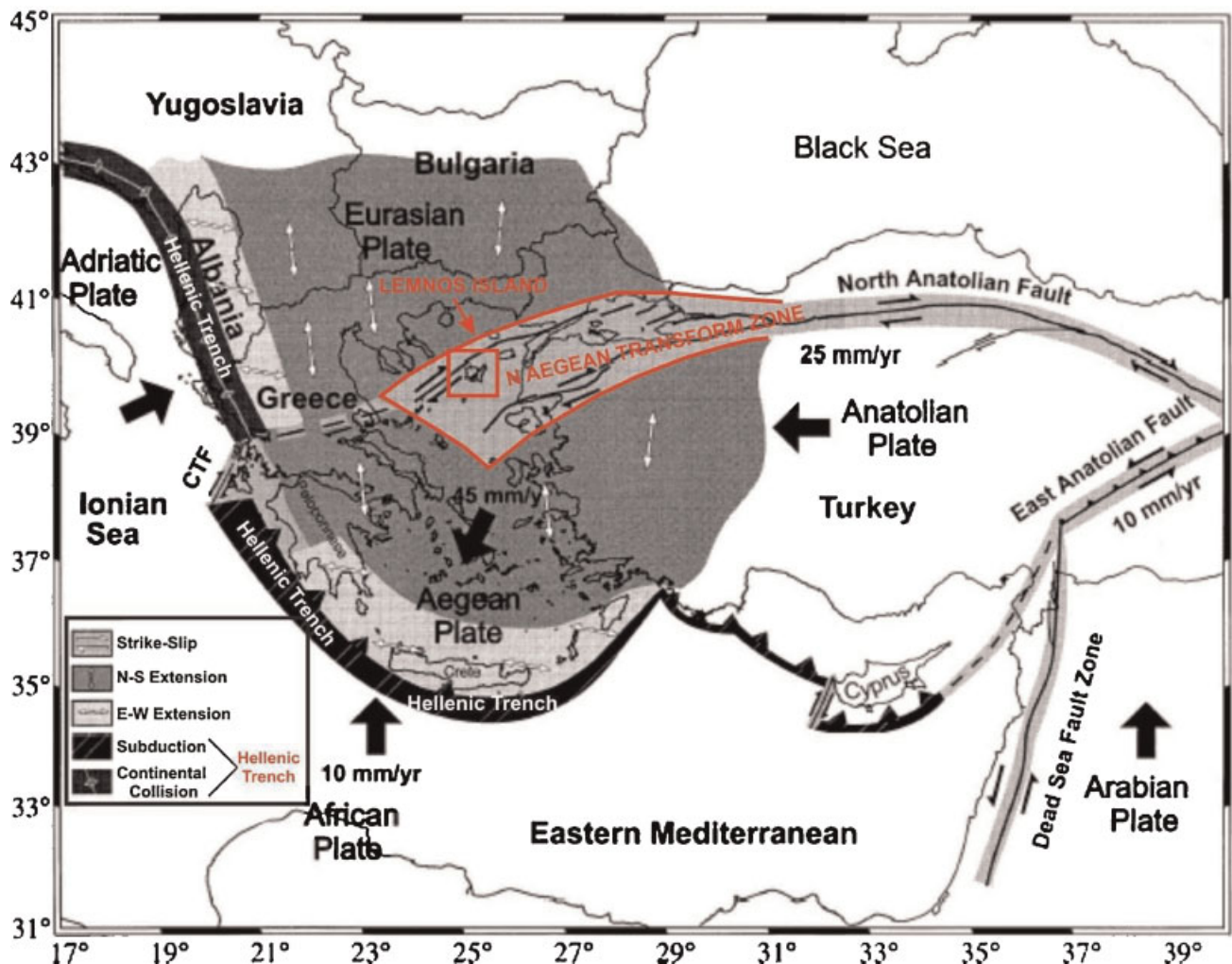


Figure 1. Plate tectonic configuration of the area around the Aegean Sea (from Papazachos *et al.* 1998).

and African plates played a key role in controlling magmatism in the Balkan Peninsula since the Late Cretaceous period. During this time, collision resulted in the formation of several subparallel southward-migrating magmatic belts with the youngest one being the present-day Aegean Arc (Fyticas *et al.* 1984). During the late Eocene–early Oligocene period, magmatic activity, as an effect of the subduction of the African Plate beneath the Eurasian Plate, occurred in the Macedonian–Rhodope–North Aegean region (Harkovska *et al.* 1989; Marchev and Shanov 1991). The magmatic belt extends to the NW into Skopje and Serbia, crossing the Vardar Zone (Bonchev 1980; Cvetkovic *et al.* 1995) and continues to the SE in the Thracian basin and Western Anatolia (Yilmaz and Polat 1998; Aldanmaz *et al.* 2000). A subduction mechanism has been proposed to explain late Cretaceous magmatism in the Rhodope Zone (Dabovski 1991). High-precision U–Pb zircon and rutile age dating in the Central Rhodope area (Peytcheva *et al.* 2002) document a southward shift of this magmatism from 92 to 78 Ma. The progressive southward migration of magmatic activity in the Aegean region (Fyticas *et al.* 1984) that commenced in the Rhodope in the Late Eocene (Yanev *et al.* 1998), has been confirmed by seismic tomography (Spakman *et al.* 1988), implying that present day north-vergent subduction in the Aegean region started by at least 40 Ma. It is generally believed that extension in the Greek part of the Rhodope Zone started not earlier than the Early Miocene (Dinter and Royden 1993; Dinter 1994; Dinter *et al.* 1995). The Aegean region has experienced back-arc extension, related to the Hellenic subduction system, since the latest Oligocene to the present (McKenzie 1978; Le Pichon and Angelier 1979; Meulenkamp *et al.* 1988), while back-arc extension in the Aegean area was (apparently) initiated between 15 and 20 Ma ago (Angelier *et al.* 1982; Jolivet *et al.* 1994). The extension started to be modified about 5 Ma ago, after the North Anatolian Fault had started to open the Sea of Marmara pull-apart basin and crossed the Dardanelles (Armijo *et al.* 1999). If this is true, the formation of sedimentary basins in the NE Aegean Sea (e.g. Lemnos Island), and the Oligocene magmatic activity in the Rhodope area, may be related to compression rather than to extension. The presence of large-scale anticlines, in the north and northeastern parts of the study area, confirms the NE Aegean Sea compressional regime.

During this time interval (Biozones NP18–Np21b, according to Martini's [1971] classification) the studied area was characterized by the deposition of submarine fans that underlay shelf deposits, with tectonic activity being responsible for this upward shallowing of the depositional environment (Maravelis *et al.* 2007). Turbidites, deposited from the inner and outer parts of a submarine fan system,

consist of alternating sandstone and mudstone beds. Sandstones occur in both complete and incomplete Bouma sequences. According to Maravelis *et al.* (2007) the turbidity system is structured by a 'basin floor' fan that is presented underlying a 'slope' fan, and was constructed under the synchronous interaction of both progradation and aggradation processes. 'Basin floor' fan is the more distal and lower positioned, unchannelized fan and is composed of lobe, lobe–fringe and fan–fringe deposits. The 'slope fan' consists of channel–overbank deposits, demonstrating greater proximity to the source area (Maravelis *et al.* 2007). Both 'basin floor' and 'slope' fans constitute the lower parts of the stratigraphic succession in the studied area, and have been interpreted as parts of a sand-rich submarine fan, on the base of slope to basin floor environment (Maravelis *et al.* 2007). During the Miocene, the island of Lemnos was the site of volcanic activity and magmatic rocks overlay the shelf deposits (Pe-Piper and Piper 2001). Magmatic rocks consist of both plutonic and volcanic rocks, and cover a large part of the studied area. The end of the Miocene is characterized by the sedimentation of conglomerates, marls and calcareous sandstones. Local Pleistocene porous calcareous and locally oolitic limestones and Holocene alluvial, coastal deposits and dunes are found (Figure 2).

CENOZOIC	HOLOCENE		ALLUVIUM
	PLEISTOCENE		
	PLIOCENE	LATE	SHALLOW WATER DEPOSITS
		EARLY	
	MIOCENE	LATE	VOLCANIC ROCKS
		MID	
		EARLY	
	OLIGOCENE	LATE	TURBIDITES
		EARLY	
		LATE	
EOCENE	MID		
	EARLY		
PALEOCENE	LATE		
	EARLY		

Figure 2. Generalized stratigraphic column of the Lemnos Island.

3. SAMPLING AND ANALYTICAL TECHNIQUES

Samples for modal analysis and bulk-rock geochemistry were selected in order to cover both the entire stratigraphic succession (Figure 3) of the studied area and the lateral extent of the sedimentary units (Figure 4). Thirty samples were collected, prepared and examined under a polarizing microscope. Framework mineral composition (modal analysis) was quantified using the point-counting method of Gazzi–Dickinson, as described by Ingersoll *et al.* (1984). Major elements and 14 trace elements were determined using a *Thermo Jarrell-Ash ENVIRO II ICP* plasma mass spectrometer (ICP-OES), while REE and additional ultra-trace elements were determined using a *Perkin Elmer SCIEX ELAN 6000* (ICP-MS). Bulk-rock geochemistry study was conducted on 28 sandstone and mudstone samples at the Activation Laboratories, Ontario, Canada. Two additional samples, from the base of the ‘basin-floor’ fan (of non-turbiditic origin), were selected for the bulk-rock geochemistry study. Instrumentation and sample preparation techniques are described by Hoffman (1992).

4. PETROGRAPHIC MODAL ANALYSIS

The provenance of clastic rocks has been determined by several petrographical methods, including quartz grain types

(based on undulosity and polycrystallinity (Basu *et al.* 1975; Young 1976)), and rock fragment typologies (Pettijohn *et al.* 1987). Petrographic analysis of the selected samples in this study shows that the sandstones are lithic arenites, using the classification scheme of Pettijohn *et al.* (1973) (Figure 5). The major components of the Lemnos Island sandstones are: quartz and feldspar grains, accessory and heavy minerals, metamorphic, sedimentary and igneous rock fragments. Using the Gazzi–Dickinson method, and according to the Arribas *et al.* (2000) classification scheme, these grains types are tabulated using the following main categories.

4.1. Quartz

Quartz is the most abundant component in the sandstones of the Lemnos Island and accounts for 40–58.4% of the grains (Table 1). Both monocrystalline quartz (Qm) and polycrystalline quartz (Qp) occur throughout the succession (Figure 6A). This fact suggests derivation from both granitic and gneissic sources, as well as derivation from schists, respectively (Tortosa *et al.* 1991). Monocrystalline quartz contains both nonundulose and undulose grains (Figure 6B). Nonundulose quartz grains are dominant in sandstones, derived from plutonic rocks, while monocrystalline quartz from low-rank metamorphic rocks contains both nonundulose and undulose grains (Basu *et al.* 1975).

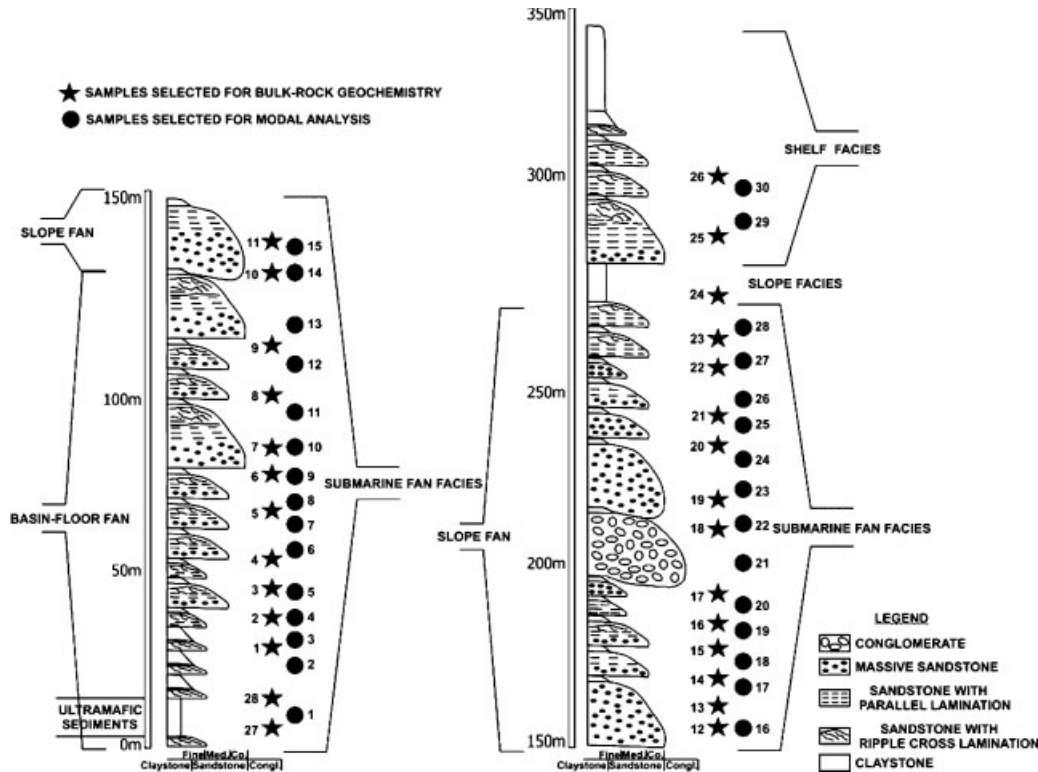


Figure 3. Stratigraphic column of the studied area.

PETROGRAPHY AND GEOCHEMISTRY SUBMARINE FANS, LEMNOS ISLAND

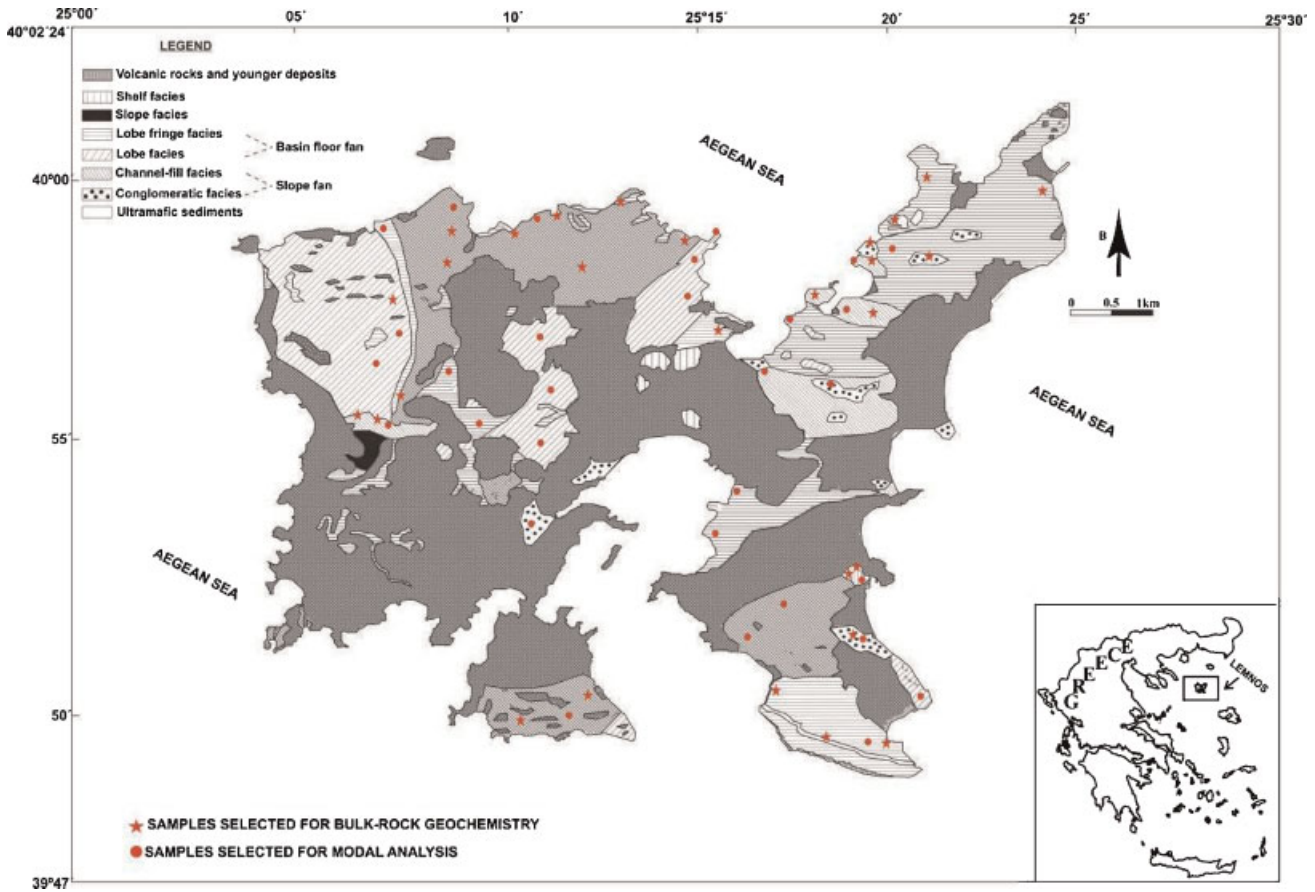


Figure 4. Geologic map of the Lemnos Island, where the selected samples are presented.

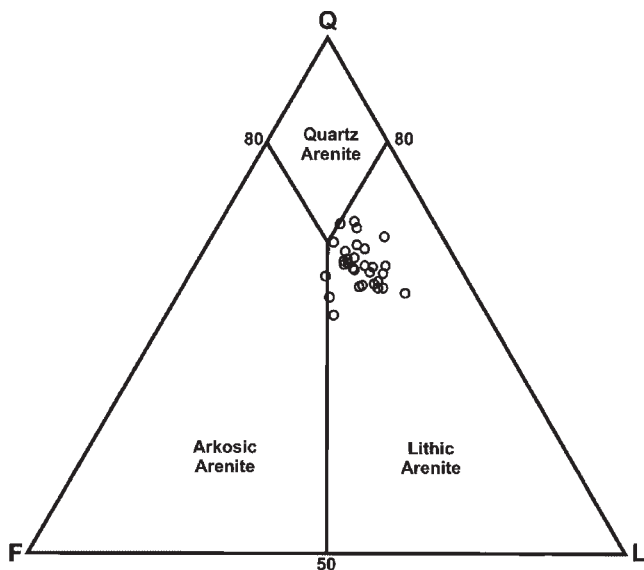


Figure 5. QFL diagram, with Pettijohn *et al.* (1973) fields.

Quartz grains may or may not have inclusions. When present, the most common inclusion is zircon, suggesting a plutonic igneous origin (Morton 1985; Morton *et al.* 1992). Qm is usually in the form of subangular to subrounded and occasionally well-rounded grains indicating the reworked sedimentary origin. Most of the polycrystalline quartz grains (Qp) consist of more than three crystals and have been grouped in two types: (1) polycrystalline grains, composed of more than five elongated crystals, exhibiting irregular to crenulated inter-crystal boundaries (Figure 7A) and (2) polycrystalline quartz grains, composed of five or more crystals, with straight to slightly curved inter-crystal boundaries (Figure 7B).

The first type indicates an origin from metamorphic source rocks (Blatt *et al.* 1980; Asiedu *et al.* 2000), while the second type suggests an origin from plutonic igneous rocks (Folk 1974; Blatt *et al.* 1980). Polycrystalline quartz grains with a bimodal crystal size distribution were also noticed (Figure 8). Such bimodal crystal size quartz grains can be related to a gneissic source (Blatt *et al.* 1980; Abdel-Wahab 1992).

Table 1. Modal analysis data of the selected sandstone samples

Sample No.	Qt	L	F	Sample No.	Qt	L	F	Sample No.	Qt	L	F
1	58.4	19.5	18.1	11	54	19.5	11.5	21	42.3	25	23.7
2	54.7	18.3	11.3	12	53	31.3	15.3	22	40	20	20
3	53.3	28	14	13	51	25.2	14.5	23	47.4	26.3	10.5
4	54	23	17	14	50.3	20.7	22	24	45.6	28.1	14
5	53.1	24.3	8.5	15	50	22	11.9	24	48.8	26	14
6	52.9	16.2	13.2	16	49.5	21.7	14.7	26	48.8	28.7	15
7	50.7	32.3	14.7	17	49.7	21.7	16.3	27	49.3	20.5	16.4
8	53.2	20.8	16	18	47.7	27.7	12	28	48.3	22.7	15.7
9	52.1	24.8	16.9	19	49.6	21.3	17	29	48.6	35.7	11.4
10	51.3	21	13	20	49.6	27.6	17.3	30	47	26	17

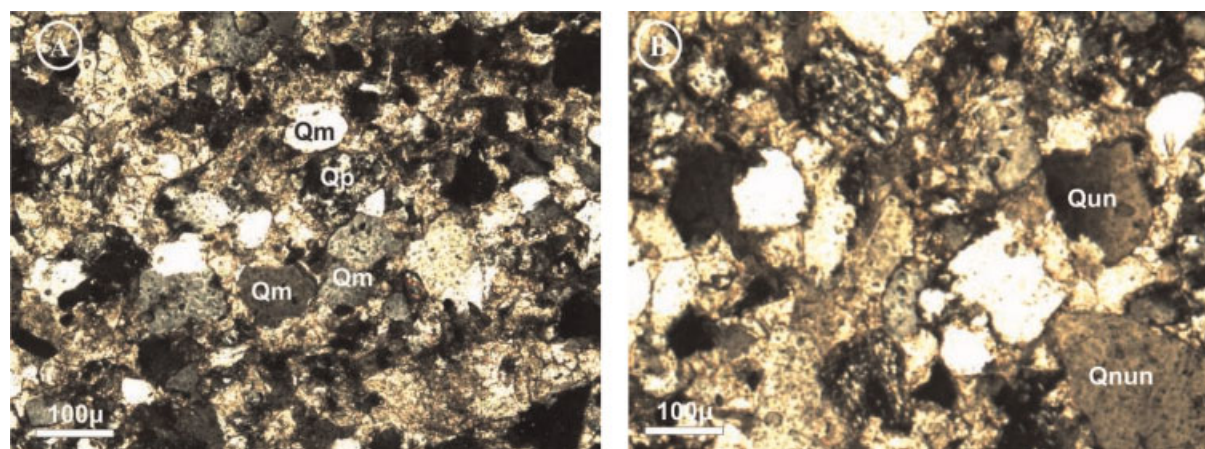


Figure 6. Photomicrographs of a lithic arenite of the Lemnos Island consisting of (A) both monocrystalline and polycrystalline quartz grains, and (B) nonundulose and undulose grains.

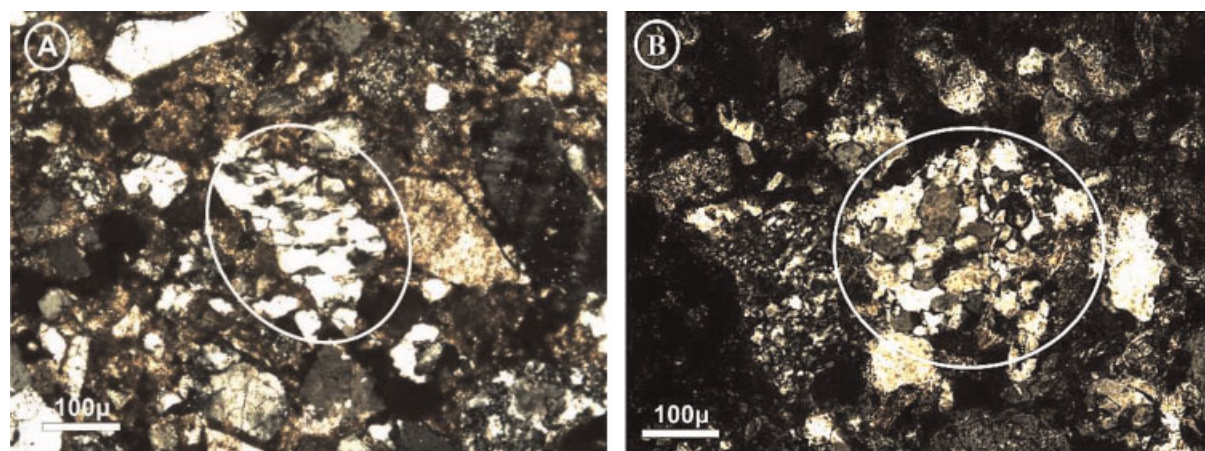


Figure 7. (A) Polycrystalline quartz grain consisting of elongated individual crystals that display crenulate to suture inter-crystal boundaries and (B) polycrystalline quartz grain exhibiting a number of individual crystals with straight to slightly curved inter-crystal boundaries.

4.2. Feldspar

Feldspar is an abundant mineral in the sandstones of the Lemnos Island, accounts for 10.5–23.7% of the grains, and consists of both alkali feldspar and plagioclase grains. Feldspar grains may be unaltered but usually they are altered

to sericite. Of these, alkali feldspar, particularly orthoclase, is the most common. Orthoclase grains are usually untwinned but simple twinning is observed in some cases (Figure 9A). Alkali feldspar may or may not have inclusions. When present, the most common inclusion is zircon suggesting a plutonic igneous origin (Morton 1985; Morton

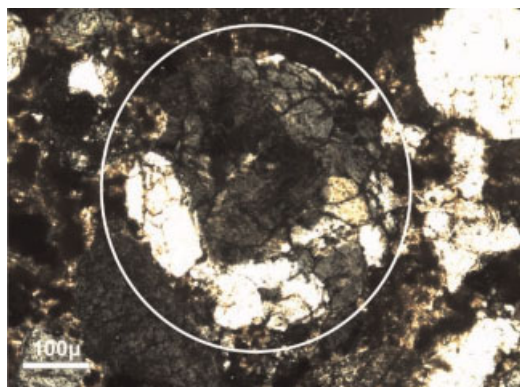


Figure 8. Polycrystalline quartz grain that displays a bimodal size distribution of individual crystals.

et al. 1992). Twinning according to the 'Albite Twin Law' is often observed in plagioclase (Figure 9B).

4.3. Lithic fragments

After quartz, lithic fragments are the most abundant component in the sandstones of the Lemnos Island, and account for 16.2–35.7% of the grains (Table 1). This category includes only fine-grained (aphanitic) fragments, because the coarse-grained (phaneritic) were not counted as rock fragments, but assigned to their respective monomineralic categories (i.e. quartz, feldspars) depending on which crystal was encountered at the cross hair. A wide range of fragments has been observed in thin sections including metamorphic (Lm), sedimentary (Ls) and igneous (Li) lithic fragments. Metamorphic fragments consist of schist rock fragments, while sedimentary lithic fragments include those of microcrystalline chert and sandstone rock fragments. The igneous lithic fragments consist of felsic plutonic granite and mafic volcanoclastic basalt fragments (Figure 10).

4.4. Heavy minerals

A limited range of heavy minerals has been observed in thin sections. The most common are well-rounded, green/brown rutiles and tourmalines (Figure 11). Their occurrence suggests an origin from igneous (plutonic) source rocks (Morton 1985; Morton *et al.* 1992).

4.5. Accessory minerals

The accessory minerals that have been identified in the sandstones of the Lemnos Island include apatite, biotite, muscovite, chlorite and glauconite grains.

4.6. Summary

The determination of the tectonic setting of sandstones using the framework mineral composition (detrital modes) was first proposed by Crook (1974), and has since undergone considerable refinement (e.g. Dickinson and Suczek 1979; Dickinson *et al.* 1983). Modal analysis from point-counting of the framework grains is listed in Table 1, where total quartz (Q_t), total feldspar (F) and total lithic fragments (L) are distinguished. Plotting data, from the modal analysis of the Lemnos sandstones, in the ternary $Q_t FL$ diagram, of Dickinson *et al.* (1983), shows that the selected sandstones cluster entirely in the recycled orogen field (Figure 12). This fact, according to the Dickinson and Suczek (1979) model, could be related to a subduction complex provenance, for the studied area.

5. TECTONIC SETTING BASED ON MAJOR, TRACE AND RARE EARTH ELEMENTS

5.1. Major element chemistry

The major element chemistry, of the selected samples (Table 2), is discussed in terms of discrimination diagrams,

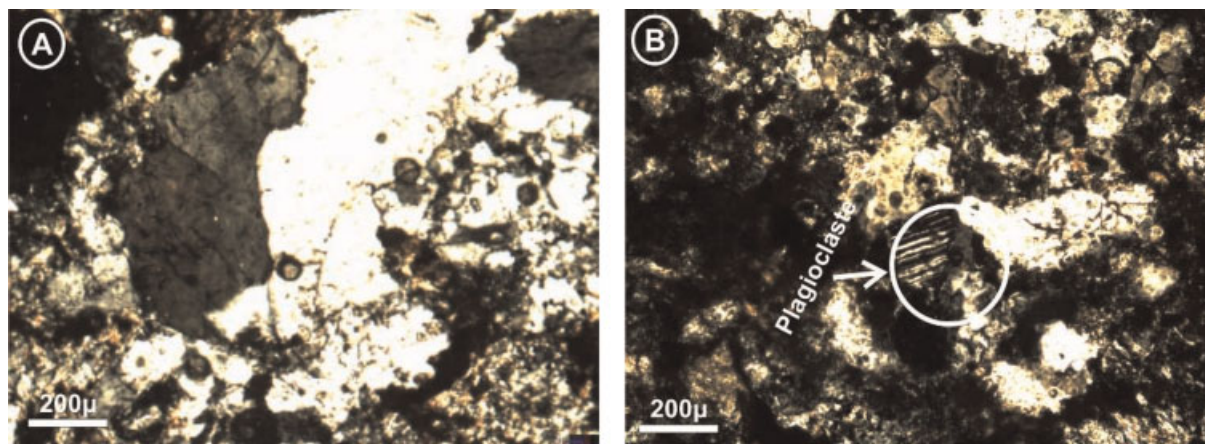


Figure 9. Photomicrographs of the selected samples of the Lemnos Island. (A) K-feldspar and (B) Plagioclase grains.

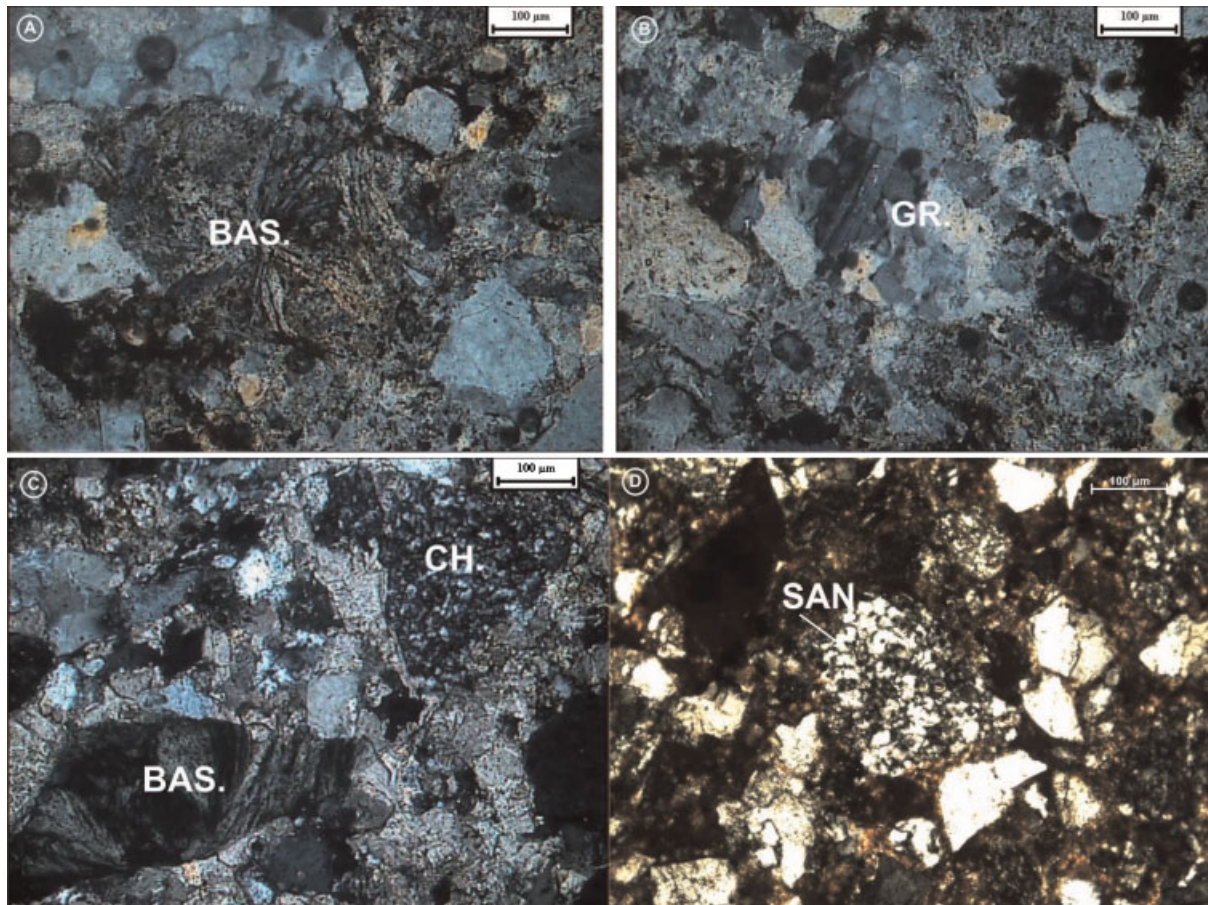


Figure 10. Photomicrographs of lithic fragments identified within the selected sandstone samples of Lemnos Island. (A) Basalt rock fragment (BAS). (B) Granite (GR). (C) Basalt (BAS) and Chert (CH). (D) Sandstone rock fragment (SAN).

used to characterize tectonic setting, proposed by Bhatia (1983); Roser and Korsch (1986, 1988) and Maynard *et al.* (1982). These diagrams show that the selected, late Eocene–early Oligocene, sandstone and mudstone samples plot in the active continental margin/continental island arc field.

Bhatia (1983) proposed that the optimum discrimination of sandstones, representing the various tectonic settings, is achieved by the plots of $\text{Fe}_2\text{O}_3 + \text{MgO}$ versus TiO_2 , $\text{Al}_2\text{O}_3/\text{SiO}_2$ and $\text{K}_2\text{O}/\text{Na}_2\text{O}$ (Figure 13A, B and C). These plots demonstrate that the sandstones derived from the Lemnos

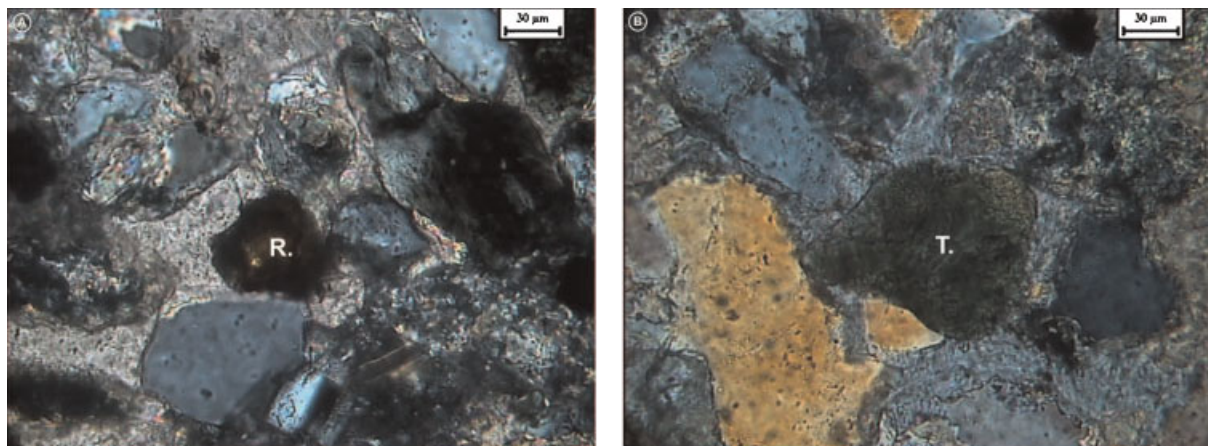


Figure 11. Photomicrographs showing (A) rutile and (B) tourmaline grains within the lithic arenites of the Lemnos Island.

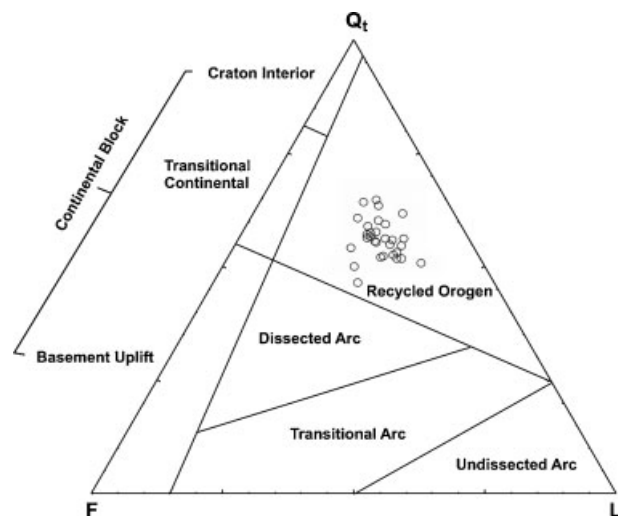


Figure 12. QFL diagram, with fields of Dickinson *et al.* (1983). All the sandstones fall in the Recycled Orogen provenance field.

Island cluster in the active continental margin and in the continental island arc fields.

Roser and Korsch (1986) have developed a bivariate tectonic discriminator that uses SiO_2 contents and $\text{K}_2\text{O}/\text{Na}_2\text{O}$ ratios, for both sandstones and mudstones. The fields are based on ancient sandstone–mudstone pairs, cross-checked against modern sediments from known tectonic

settings. With this, these authors were able to differentiate between sediments derived from volcanic island arcs (ARC), active continental margins (ACM) and passive continental margins (PM). Associated with subduction zones, ARC-derived material is typical of fore-arc, back-arc and inter-arc basins formed on oceanic crust. ACM-derived material occurs in similar settings but on continental crust. PM sediments are derived from stable continental areas and deposited in intra-cratonic basins or on passive continental margins. Application of this particular discrimination diagram demonstrates that most of the selected samples cluster in the active continental margin field, while a few samples cluster in the passive margin field (Figure 14).

Maynard *et al.* (1982) used a similar plot of $\text{K}_2\text{O}/\text{Na}_2\text{O}$ versus $\text{SiO}_2/\text{Al}_2\text{O}_3$ to discriminate different tectonic settings, in their study of modern sediments (Figure 15). In this plot, data from the late Eocene–early Oligocene samples on the studied area fall mainly into the A2 field (evolved arc setting, felsitic–plutonic detritus) and into the active continental margin (ACM) field.

Floyd and Leveridge (1987) and McCann (1991) used a K_2O versus Rb plot to distinguish sediments derived from acid to intermediate rock compositions from those derived from basic rock composition. As seen in Figure 16 the majority of the sandstone samples have a K/Rb ratio that lies close to a typical differentiated magmatic suite or ‘main trend’ with the ratio of 230 (Shaw 1968). This feature, in

Table 2. Major and minor oxide values of the selected samples. Values are quoted in weight % recalculated 100% loss on ignition (LOI) free

Sample ID	$\text{SiO}_2\%$	$\text{Al}_2\text{O}_3\%$	$\text{Fe}_2\text{O}_3(\text{T})\%$	MnO%	MgO%	CaO%	$\text{Na}_2\text{O}\%$	$\text{K}_2\text{O}\%$	TiO ₂ %	P ₂ O ₅ %	LOI%
1 (mudstone)	69.608	15.402	7.9558	0.0318	1.3259	0.73	1.0183	2.69	0.7934	0.1591	5.73
2 (sandstone)	65.897	8.0617	3.8046	0.3247	1.1947	17.7	1.6587	1.20	0.4384	0.1159	13.7
3 (mudstone)	69.858	14.308	10.830	0.0644	1.1163	0.17	0.4186	3.26	0.7674	0.1288	6.84
4 (sandstone)	65.534	8.3255	5.0465	0.0930	4.3953	11.8	2.3255	1.63	0.5383	0.1395	14
5 (mudstone)	62.471	15.162	6.2922	0.0787	3.7595	7.57	1.6434	3.01	0.8250	0.1463	11.1
6 (sandstone)	64.960	8.3101	3.4818	0.2089	2.3909	16.6	1.7061	1.86	0.4886	0.1044	13.8
7 (sandstone)	56.898	10.489	4.8740	0.4826	3.2258	18.8	1.7070	1.86	0.6934	0.1530	15
8 (mudstone)	64.250	13.267	7.3256	0.0658	4.2613	6.43	2.0757	2.10	0.7644	0.1427	8.95
9 (mudstone)	78.435	12.356	0.9094	0.0227	1.1594	2.30	3.6830	2.02	0.1705	0.0341	12.0
10 (sandstone)	68.777	12.869	6.7276	0.0958	5.2267	2.54	1.9161	1.74	0.9718	0.1809	6.06
11 (mudstone)	60.882	18.534	7.1495	0.0819	3.2880	4.77	1.1818	3.46	0.9431	0.1404	14.5
12 (sandstone)	74.003	10.286	6.1148	0.1097	0.4940	5.93	0.0878	1.36	0.6455	0.1317	8.91
13 (sandstone)	79.276	11.882	3.4787	0.0212	0.6489	2.26	0.1170	1.70	0.7414	0.1489	6
14 (mudstone)	65.877	19.808	4.0725	0.0217	1.4443	1.02	1.7267	3.77	1.1424	0.1737	7.92
15 (mudstone)	67.794	18.266	5.5090	0.0536	1.0309	1.03	0.9020	3.33	1.0631	0.1932	6.88
16 (sandstone)	60.920	8.1678	2.8415	0.2972	1.5337	21.1	1.7833	2.17	0.5255	0.1070	15.8
17 (sandstone)	68.936	9.9003	6.3455	0.0996	1.3953	8.23	2.0819	2.02	0.5681	0.1107	9.7
18 (sandstone)	69.323	6.4843	3.5486	0.0943	2.3697	15.3	2.0160	1.15	0.3607	0.0707	15.1
19 (mudstone)	46.370	14.666	7.2465	0.1364	3.0276	21.5	1.4766	2.72	0.7283	0.1613	19.4
20 (sandstone)	70.140	7.8326	4.2412	0.0684	1.0261	14.0	1.2883	1.67	0.4070	0.1026	12.2
21 (sandstone)	71.783	11.645	5.7686	0.0756	1.6960	4.11	2.9167	2.20	0.6557	0.1188	7.43
22 (sandstone)	67.550	7.3996	2.8272	0.1279	1.5125	17.6	1.6986	1.58	0.5817	0.1163	14
23 (sandstone)	69.371	7.5979	4.0634	0.0787	0.7203	13.2	1.3732	1.29	0.3748	0.1013	11.1
24 (mudstone)	55.722	16.512	7.5774	0.0791	4.6935	9.46	1.4363	3.21	0.8256	0.1470	11.5
25 (sandstone)	60.541	8.7822	4.8093	0.1107	7.1340	14.6	1.7958	1.74	0.6014	0.1230	18.7
26 (mudstone)	56.833	16.511	7.2644	0.0932	3.9062	8.69	0.9911	3.28	0.9223	0.1282	14.2

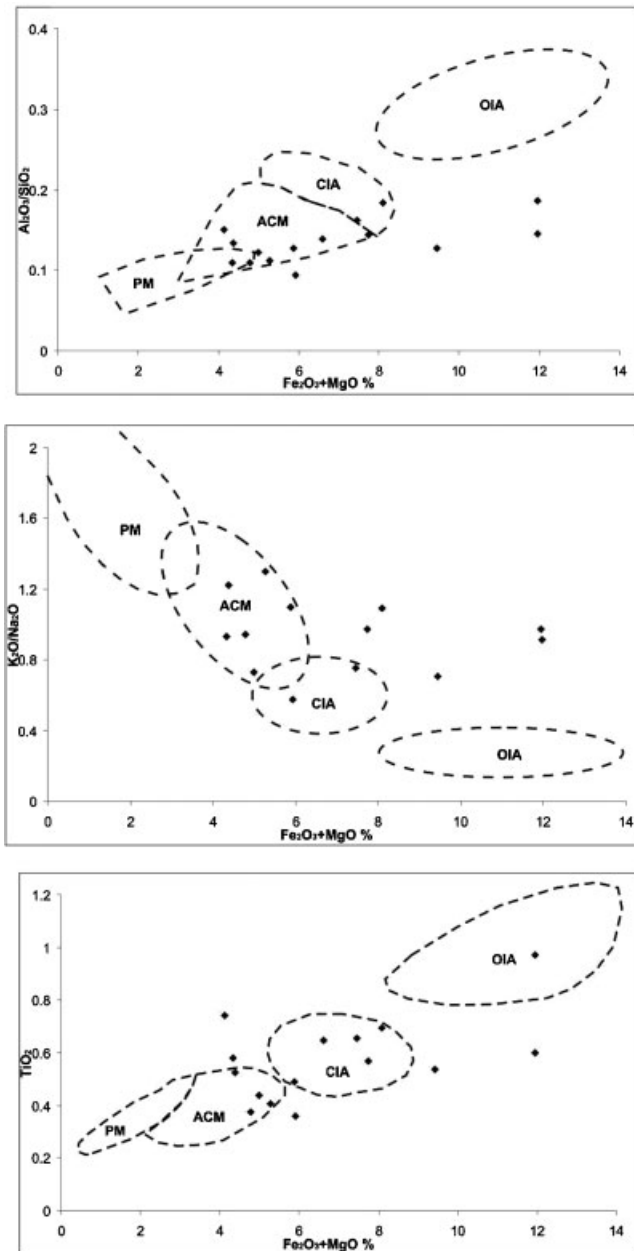


Figure 13. Plots of the major element composition of the Lemnos sandstones on the tectonic setting discrimination diagrams of Bhatia (1983). (OIA) Oceanic island Arc, (CIA) Continental island Arc, (ACM) Active continental margin, (PM) Passive margin.

association with the moderate K and Rb content, suggests that the sandstones could be the erosional products of a series of magmatic rocks, predominantly of basic composition. Compared to associated arenites, mudstones have higher contents of K_2O (average 1.68 wt% and 2.99 wt%, respectively), reflecting the greater proportions of clay minerals (mainly illite and sericite), and more mafic components in the mudstones. Mudstones are commonly enriched in most trace elements, including large ion

lithophile and ferromagnesian trace elements. These enrichments are most likely due to a combination of high concentrations of these elements in clay minerals and a dilution effect from quartz in sands (McLennan *et al.* 1990). These higher concentrations are displayed in the plot of Figure 16, where the mudstone samples seem to have been derived from magmatic rocks of acid + intermediate composition.

Both sandstone and mudstone samples display positive correlations between K versus Rb (r^2 value of 0.166 and 0.437, respectively) and K versus Cs (r^2 value of 0.0082 and 0.122, respectively) (Figure 17A, B) indicating that K-bearing clay minerals (e.g. illite and sericite) probably control the abundances of these elements (e.g. McLennan *et al.* 1983; Feng and Kerrich 1990; Gu 1994).

To sum up, the major element study of the Lemnos samples suggests that the studied area is located in an active continental margin/continental island arc environment, while a basic signature for the source is revealed. However, provenance results based on major elements, in general have to be treated with care, since alkali elements can also be highly mobile through weathering and recycling and thus can vary original provenance signatures (Roser and Korsch 1988; Bahlburg 1998).

5.2. Trace element chemistry

The trace element chemistry of the selected samples is discussed in terms of discrimination diagrams, used to characterize tectonic setting, proposed by Bhatia and Crook (1986). Trace element values of the studied sediments are presented in Table 3. Th/Sc and Zr/Sc element ratios can reveal a compositional heterogeneity in the source(s), if the samples show Th/Sc and Zr/Sc values along the trend from mantle to upper continental crust compositions (McLennan *et al.* 1993). Th/Sc ratio is a good overall indicator of igneous chemical differentiation processes since Th is typically an incompatible element, whereas Sc is typically compatible in igneous systems (McLennan *et al.* 1993). Th/Sc ratio of our samples, cluster both in the upper continental crust and the mantle compositional field (Figure 18).

Samples that display Th/Sc values below the value of average upper crust reflect input of a less evolved source to the studied sediments (Zimmermann and Bahlburg 2003). The majority of the Th/Sc values scatter around the Upper Continental Crust (UCC) average of 0.76 (McLennan 2001) apart from the sample B1 that is presented with a value (13.458) far above the UCC. The high value is a result of low concentration in Sc in association with a high concentration in Th indicating an upper crust provenance of the sample.

Zr/Sc ratio is commonly used as a measure of the degree of sediment recycling and as an index of zircon enrichment,

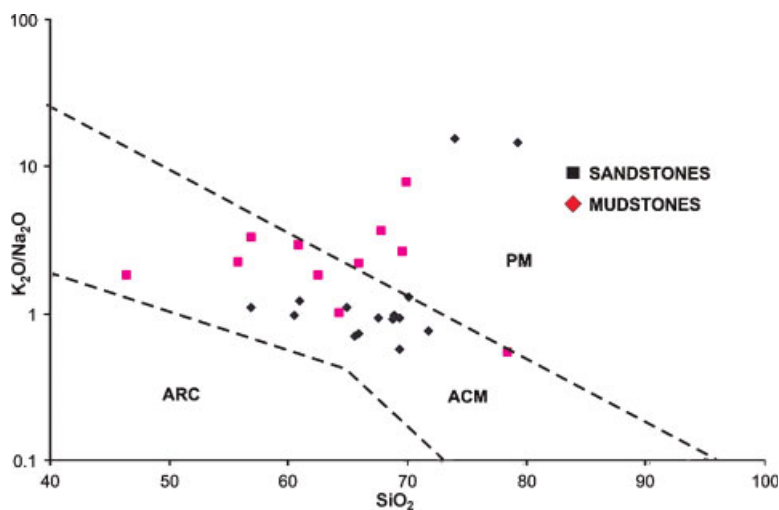


Figure 14. Geochemical discrimination plot for the studied samples, after Roser and Korsch (1986), using SiO_2 versus $\text{K}_2\text{O}/\text{Na}_2\text{O}$ to discriminate geotectonic settings of the Lemnos Island. PM, Passive margin; ACM, Active continental margin; ARC, Island Arc.

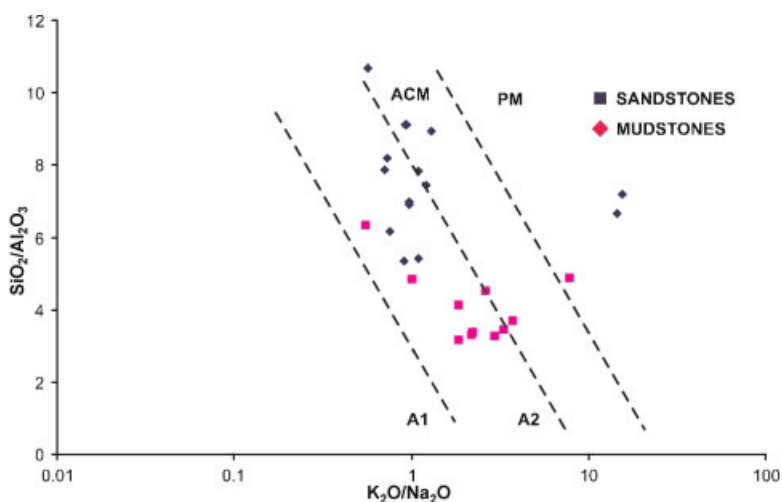


Figure 15. Plot of $\text{SiO}_2/\text{Al}_2\text{O}_3$ versus $\text{K}_2\text{O}/\text{Na}_2\text{O}$ for the selected sediments. Boundary lines for different tectonic settings from Roser and Korsch (1986). ACM, active continental margin; PM, passive margin; A1, arc setting, basaltic and andesitic detritus; A2, evolved arc setting, felsitic-plutonic detritus.

since Zr is strongly enriched in zircon, whereas Sc is not, but generally preserves a signature of the provenance similar to other REE (McLennan 1989; McLennan *et al.* 1993). The Zr/Sc values of our samples vary from 6.48 (sample D34) to 72.62 (sample D27) with a mean of 19.324. The majority of the values scatter around the UCC average of 13.57 (McLennan 2001), apart from the samples D27 and B1 that are presented with the highest values of Zr/Sc ratio (72.62 and 57.91, respectively). Sample B1 owes this high value mainly to the Sc concentration (2.4 ppm), far below the value of average upper crust (14 ppm, McLennan 2001). Sample D27, apart from the low Sc concentration (6.5 ppm), displays a high Zr concentration (443 ppm), far above the value of average upper crust (190 ppm, McLennan 2001), indicating reworking and sorting during sediment transfer (Bahlborg 1998).

Floyd *et al.* (1991) pointed out that the element ratio La/Th plotted versus the concentration of hafnium (Hf) demonstrates the degree of recycling in sandstones, and also implicates information about their provenance. A plot of La/Th versus Hf provides useful bulk rock discrimination between different arc compositions and sources (Floyd and Leveridge 1987). These trace element ratios of the Lemnos samples (Figure 19), indicate only a weak recycling, and in addition, suggest that the studied area was mostly influenced from a felsic island arc source, while a mixed felsic and mafic source has contributed during the deposition.

The plot of La versus Th proposed by Bhatia (1983) (Figure 20) shows that three broad fields representing oceanic island arc (OIA), continental island arc (CIA) and both active and passive continental margin (ACM and PM), respectively, can be recognized.

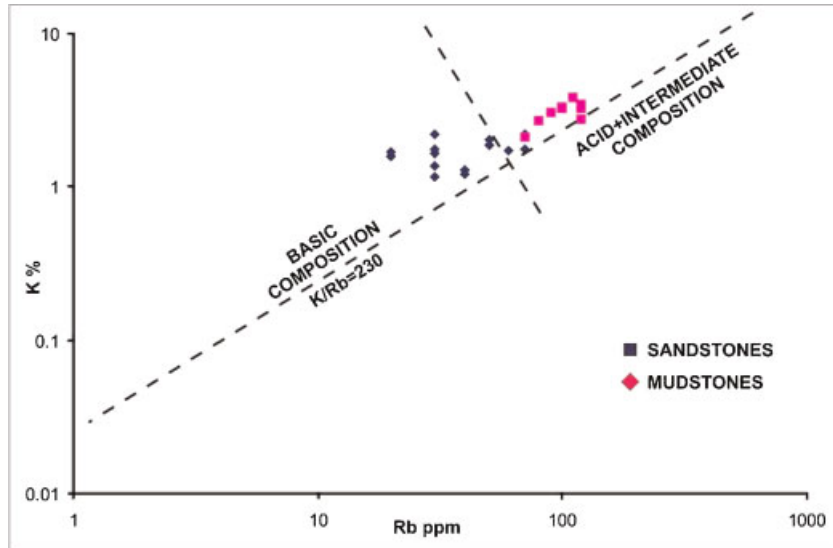


Figure 16. K_2O versus Rb plot for the discrimination of the Lemnos samples. Boundary line between acid/intermediate and basic compositions, in plot after Floyd and Leveridge (1987).

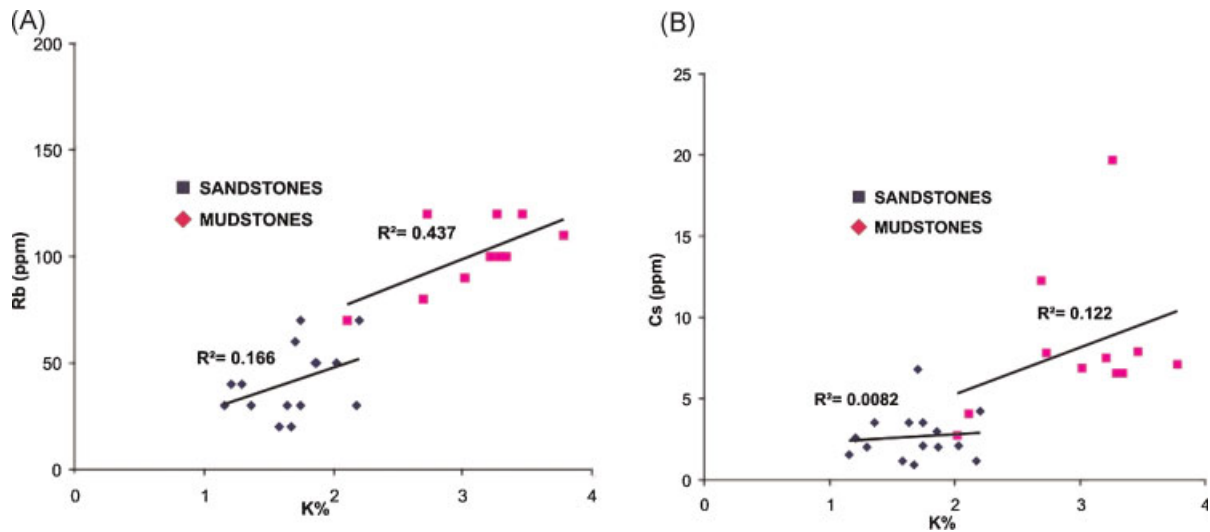


Figure 17. Plots of K versus (A) Rb and (B) Cs. Note the positive correlations for K–Rb and K–Cs.

The values of the La/Th ratios of the selected sediments oscillate between 0.975 (sample B1) and 3.517 (sample E14) with a mean value of 2.53 and reflect the influence of a magmatic arc in the hinterland (e.g. Bhatia 1985; Bhatia and Crook 1986; McLennan *et al.* 1993). In the plot of Figure 20 most of the studied samples cluster in the continental island arc provenance field (CIA), whereas the samples D9 and E14 scatter over the OIA discrimination field. This observation concurs with results given in Figure 21A and B (Th–Sc–La and Th–Sc–Zr/10 based on Bhatia and Crook 1986, respectively). The selected sediments of the Lemnos Island cluster in the continental island arc field.

Zr/Th ratio is another measure of the recycling degree (Zimmermann and Bahlburg 2003). The studied samples display Zr/Th ratios between 4.3 (sample B1) and 68.153 (sample D27), with an average of 22.85 (Table 4). The high Zr/Th value of some samples can be attributed to the reworking and sorting, during sediment transfer, resulting in high Zr values (Bahlburg 1998).

Trace elements, such as Cr, are useful in identifying accessory detrital components, such as chromite, commonly derived from mafic to ultramafic sources, including ophiolites, not readily recognized by petrography alone (Zimmermann and Bahlburg 2003). The average Cr content

PETROGRAPHY AND GEOCHEMISTRY SUBMARINE FANS, LEMNOS ISLAND

Table 3. Summary of selected trace element data for the late Eocene–early Oligocene Lemnos Island deposits

		Sandstones							
Sample	Number	2	4	6	7	10	12	13	
Au	ppb	< 5	< 5	< 5	< 5	< 5	< 5	< 5	9
Ag	ppm	< 0.5	0.9	< 0.5	< 0.5	< 0.5	< 0.5	< 0.5	< 0.5
As	ppm	15	4	6	10	21	31	98	
Ba	ppm	110	270	198	235	293	226	268	
Be	ppm	1	1	1	2	2	1	2	
Bi	ppm	< 2	< 2	< 2	< 2	< 2	< 2	< 2	
Br	ppm	< 1	< 1	< 1	< 1	1	1	2	
Cd	ppm	< 0.5	< 0.5	< 0.5	< 0.5	0.5	< 0.5	< 0.5	
Co	ppm	6	6	11	18	26	21	15	
Cr	ppm	138	236	229	211	411	266	259	
Cs	ppm	2.6	3.5	2	3	3.5	3.5	6.8	
Cu	ppm	18	13	16	22	34	25	28	
Hf	ppm	3.1	5.5	3.1	4.1	8.1	5	4.5	
Hg	ppm	< 1	< 1	< 1	< 1	< 1	< 1	< 1	
Ir	ppb	< 5	< 5	< 5	< 5	< 5	< 5	< 5	
Mo	ppm	< 2	< 2	< 2	< 2	< 2	< 2	< 2	
Ni	ppm	82	64	115	101	199	137	126	
Pb	ppm	7	7	8	10	< 5	15	16	
Rb	ppm	40	30	50	50	70	30	60	
S	%	0.006	0.011	0.01	0.003	0.004	0.007	<0.001	
Sb	ppm	0.9	0.3	0.3	0.5	0.6	9.4	10.6	
Sc	ppm	6.6	8.5	7.2	11.1	16.8	12.7	9.8	
Se	ppm	< 3	< 3	< 3	< 3	< 3	< 3	< 3	
Sr	ppm	239	756	254	204	118	104	54	
Ta	ppm	< 1	< 1	< 1	< 1	< 1	< 1	< 1	
Th	ppm	5.3	6.5	5.8	8.4	10.8	7.3	8.8	
U	ppm	1.8	1.6	2	2.6	3.2	2.9	2.6	
V	ppm	46	64	49	84	123	84	95	
W	ppm	< 3	< 3	< 3	< 3	< 3	< 3	< 3	
Y	ppm	17	20	16	21	24	23	17	
Zn	ppm	36	38	34	49	87	61	86	
Zr	ppm	144	225	140	164	389	217	174	
Sample	Number	16	17	18	20	21	22	23	25
Au	ppb	< 5	< 5	< 5	< 5	< 5	< 5	< 5	< 5
Ag	ppm	< 0.5	< 0.5	< 0.5	< 0.5	< 0.5	< 0.5	< 0.5	< 0.5
As	ppm	8	6	3	3	7	3	11	4
Ba	ppm	229	287	194	208	333	212	149	226
Be	ppm	< 1	2	1	1	2	1	1	1
Bi	ppm	< 2	< 2	< 2	< 2	< 2	< 2	< 2	< 2
Br	ppm	< 1	2	45	1	12	< 1	1	2
Cd	ppm	< 0.5	< 0.5	< 0.5	< 0.5	< 0.5	< 0.5	< 0.5	< 0.5
Co	ppm	12	21	13	13	19	10	13	9
Cr	ppm	204	208	432	183	211	763	178	168
Cs	ppm	1.2	2.1	1.6	0.9	4.2	1.2	2	2.1
Cu	ppm	12	21	11	9	24	13	14	12
Hf	ppm	3.7	3.7	3.3	2.8	3.5	8.5	2.5	4
Hg	ppm	< 1	< 1	< 1	< 1	< 1	< 1	< 1	< 1
Ir	ppb	< 5	< 5	< 5	< 5	< 5	< 5	< 5	< 5
Mo	ppm	< 2	< 2	< 2	< 2	< 2	< 2	< 2	< 2
Ni	ppm	71	150	96	90	127	65	103	76
Pb	ppm	7	13	< 5	10	16	6	9	7
Rb	ppm	30	50	30	20	70	20	40	30
S	%	0.064	0.003	0.128	0.005	0.013	0.004	0.007	0.139
Sb	ppm	0.4	0.4	0.3	0.2	0.5	0.3	1.1	< 0.2

(Continues)

Table 3. (Continued)

Sample	Number	16	17	18	20	21	22	23	25
Sc	ppm	7	12.5	6.2	6	14.3	6.1	6.2	7
Se	ppm	< 3	< 3	< 3	< 3	< 3	< 3	< 3	< 3
Sr	ppm	216	172	157	255	222	376	58	301
Ta	ppm	< 1	< 1	< 1	< 1	< 1	< 1	< 1	< 1
Th	ppm	4.5	6.6	4.6	4.4	8.9	6.5	5.3	5.3
U	ppm	2.2	2.8	1.8	1.3	1.9	1.9	1.5	1.3
V	ppm	50	81	49	43	95	38	49	48
W	ppm	< 3	< 3	< 3	< 3	< 3	< 3	< 3	< 3
Y	ppm	15	26	15	17	22	19	13	16
Zn	ppm	26	64	38	30	55	29	37	24
Zr	ppm	156	184	144	150	141	443	99	186

Mudstones												
Sample	Number	1	3	5	8	9	11	14	15	19	24	26
Au	ppb	< 5	< 5	< 5	< 5	< 5	8	< 5	5	6	< 5	< 5
Ag	ppm	< 0.5	< 0.5	< 0.5	< 0.5	1.3	< 0.5	< 0.5	0.6	0.6	< 0.5	< 0.5
As	ppm	40	19	6	17	2	7	13	11	3	9	11
Ba	ppm	374	285	300	300	950	355	389	410	266	315	308
Be	ppm	3	3	2	2	4	3	3	3	2	3	2
Bi	ppm	< 2	< 2	< 2	< 2	< 2	< 2	< 2	< 2	< 2	< 2	< 2
Br	ppm	3	9	2	3	4	7	17	3	3	< 1	3
Cd	ppm	< 0.5	0.7	< 0.5	< 0.5	< 0.5	< 0.5	< 0.5	< 0.5	< 0.5	0.5	< 0.5
Co	ppm	21	22	13	26	< 1	20	12	16	25	26	21
Cr	ppm	194	201	229	215	18	197	265	270	166	185	196
Cs	ppm	12.3	19.7	6.9	4.1	2.7	7.9	7.1	6.6	7.8	7.5	6.6
Cu	ppm	61	44	38	32	4	50	55	53	35	46	41
Hf	ppm	4.3	3.2	4	3.7	3.7	2.9	4.2	4.6	2.4	2.7	3.7
Hg	ppm	< 1	< 1	< 1	< 1	< 1	< 1	< 1	< 1	< 1	< 1	< 1
Ir	ppb	< 5	< 5	< 5	< 5	< 5	< 5	< 5	< 5	< 5	< 5	< 5
Mo	ppm	< 2	< 2	< 2	< 2	< 2	< 2	< 2	< 2	< 2	< 2	< 2
Ni	ppm	246	129	158	147	18	132	78	117	144	154	148
Pb	ppm	15	23	13	21	21	17	17	10	16	17	15
Rb	ppm	80	120	90	70	< 20	120	110	100	120	100	100
S	%	0.009	0.012	0.001	0.215	0.062	0.113	0.014	0.005	0.014	0.723	0.055
Sb	ppm	3.9	5.9	0.4	0.5	< 0.2	0.6	0.6	0.5	0.5	0.6	0.5
Sc	ppm	19.6	18.5	15.6	11.9	2.4	17.5	16.7	14.7	14.3	17.9	17.5
Se	ppm	< 3	< 3	< 3	< 3	< 3	< 3	< 3	< 3	< 3	< 3	< 3
Sr	ppm	57	163	201	196	983	257	320	350	588	213	217
Ta	ppm	1	< 1	< 1	< 1	2	2	2	1	1	< 1	< 1
Th	ppm	10.6	11.6	11.3	7.9	32.3	12.6	14.3	13.4	9.7	12.1	12.1
U	ppm	3.3	4.2	3.4	2.3	12.6	4.2	4.2	3.8	2.4	2.8	3
V	ppm	145	172	121	123	10	152	157	140	123	153	137
W	ppm	< 3	< 3	< 3	< 3	< 3	< 3	4	< 3	< 3	< 3	< 3
Y	ppm	27	25	23	21	20	20	20	22	17	23	26
Zn	ppm	148	122	71	62	26	63	58	72	73	81	78
Zr	ppm	175	141	161	171	139	129	168	189	97	116	157

Samples From the Base of the Basin–Floor Fan

Sample ID	Au ppb	Ag ppm	As ppm	Ba ppm	Be ppm	Bi ppm	Br ppm	Cd ppm
O1	< 5	<0.5	< 2	< 3	< 1	< 2	2	<0.5
O2	< 5	<0.5	2	5	< 1	< 2	< 1	<0.5
O1	Ni ppm 1990	Pb ppm 6	Rb ppm < 20	S % 0.03	Sb ppm <0.2	Sc ppm 9.9	Se ppm < 3	Sr ppm < 2
O2	1890	< 5	< 20	0.009	<0.2	11.2	< 3	3
	Co ppm	Cr ppm	Cs ppm	Cu ppm	Hf ppm	Hg ppm	Ir ppm	Mo ppm

(Continues)

Table 3. (Continued)

Samples From the Base of the Basin–Floor Fan								
Sample ID	Au ppb	Ag ppm	As ppm	Ba ppm	Be ppm	Bi ppm	Br ppm	Cd ppm
O1	101	2220	<0.5	3	<0.5	< 1	< 5	< 2
O2	97	2190	<0.5	3	<0.5	< 1	< 5	< 2
	Ta ppm	Th ppm	U ppm	V ppm	W ppm	Y ppm	Zn ppm	Zr ppm
O1	< 1	<0.5	<0.5	30	< 3	< 1	28	< 2
O2	< 1	<0.5	<0.5	39	< 3	< 1	40	< 2

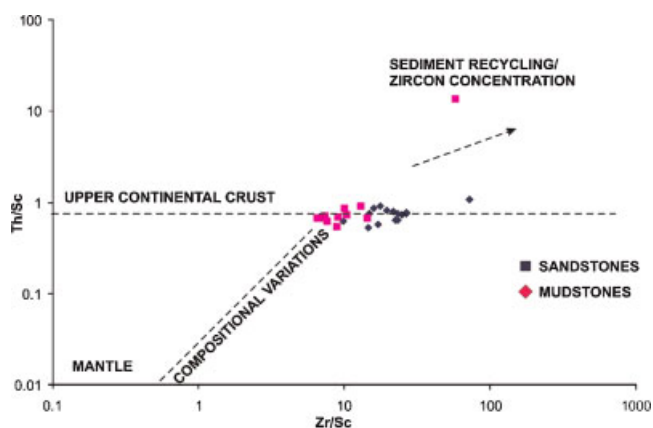


Figure 18. Plot of Th/Sc versus Zr/Sc for the studied sediments. Note the distribution of significant number of samples in the mantle compositional field reflecting input of a less evolved source.

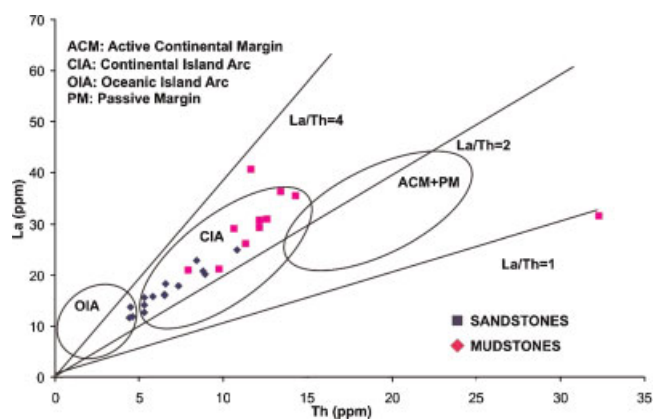


Figure 20. La versus Th diagram displaying provenance fields after Bhatia (1983).

of the upper continental crust is 83 ppm (McLennan 2001). The respective values of the studied sediments (Table 4) vary from 18 ppm (sample B1) to 432 ppm (sample D27), with an average value, for the late Eocene–early Oligocene sediments, of 280 ppm, far above the UCC value of 83 ppm (McLennan 2001). This high and variable Cr content is probably a reflection of changing source composition, and the incoming of detrital material of

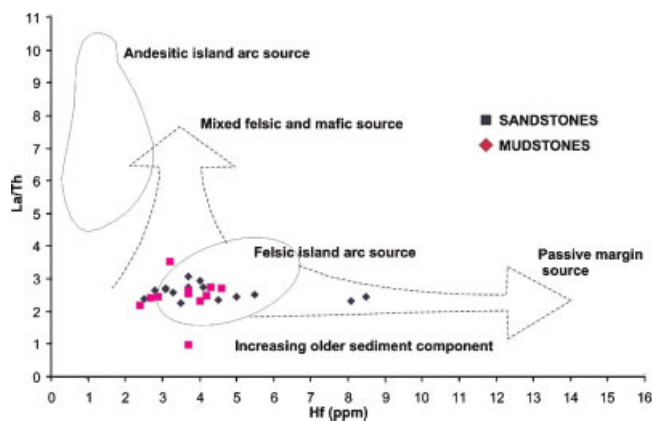


Figure 19. Source and compositional discrimination of the selected samples, in terms of La/Th ratio and Hf abundance. Note the great importance of the felsic island source in relation to the mixed felsic/mafic and passive margin source contribution.

intermediate/basic character (Floyd and Leveridge 1987). Input from mafic sources would also result in an enrichment of V and Ni. The respective values are in general much higher than in the upper continental crust, leading to relatively high Cr/V (due to high concentration in Cr) and low Y/Ni ratios in most of the samples (Table 4). This underlines the significance of a mafic or ultramafic contribution to the deposits (Floyd and Leveridge 1987; McLennan *et al.* 1993).

The incoming of detrital material of basic character is also suggested from the trace element chemistry of the samples selected from the base of the ‘basin floor’ fan (Table 3). The abundances of Cr, Ni and Co, of the two selected samples, far above the UCC values, suggest a mafic or ultramafic provenance to the deposits.

In summary, the trace element study suggests an active continental margin/continental island arc character for the late Eocene–early Oligocene of Lemnos Island. Moreover, processes like reworking and sorting were of great importance during sedimentation, in contrast to recycling, while a mixed felsic and basic/ultra basic source composition is indicated. Taking into account only bulk-rock chemistry results, it is difficult to discriminate active continental margin and island arc provenances (see discussion in Bock *et al.* 2000 and definitions in Bhatia

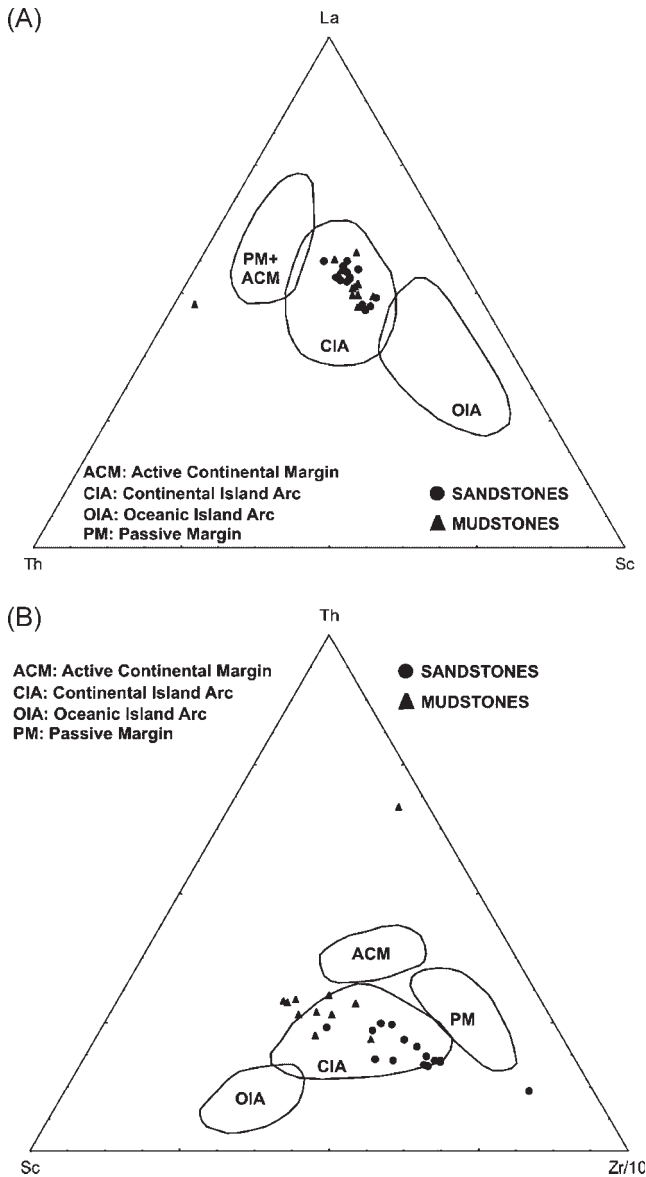


Figure 21. (A) La–Th–Sc diagram picturing provenance fields after Bhatia and Crook (1986). (B) Th–Sc–Zr/10 diagram picturing provenance fields after Bhatia and Crook (1986).

and Crook 1986). Therefore, in the Discussion section below, the petrography and mineral chemistry results are discussed in detail.

5.3. Rare earth element distribution

The abundances of eight REE (La, Ce, Nd, Sm, Eu, Lu, Tb and Yb) were determined, for 26 sandstone and mudstone samples from the Lemnos Island. The results of this analysis are shown in Table 5.

Due to the fact that the majority of the selected sediments display Tb values, lower than the detection limit of 0.5 ppm

(except for samples D3, D4, D13, D14, D33, E10 and E14), the particular REE has not been plotted in the chondrite-normalized REE plot in Figure 22.

In this diagram the mean values of the sandstone and mudstone samples have been plotted separately. All the samples are LREE enriched, relative to HREE with flat HREE patterns, and display positive Eu anomalies (Eu/Eu^* values > 1). This Europium enrichment may be explained by sedimentary processes. Plagioclase is slightly concentrated in the sandstones, by sorting (McLennan 1989) and appears to be related to high normative plagioclase content, due to a local accumulation of feldspar during sedimentation (Nance and Taylor 1977). This fact suggests that the processes of intracrustal differentiation (involving plagioclase fractionation) were not of great importance (McLennan *et al.* 1990).

The multi-element diagrams, given in Figure 23, display the element concentrations of Lemnos sandstones, normalized to the continental upper crust composition, published by Taylor and McLennan (1985) on an element-by-element basis. This procedure allows the direct comparison of element patterns to various provenance settings (e.g. Bhatia and Crook 1986; Floyd *et al.* 1991). The elements are arranged from left to right, in order of decreasing ocean residence time, and consist of a potentially mobile group (K–Ni) and a more immobile group (Ta–Th).

The analysis of Lemnos Island sandstones, in Figure 23, shows the following:

- The relative abundances of V, Cr, Ni and Ti, are > 1 , indicate a mafic input, typical of an active margin tectonic setting. Sc is presented with a positive anomaly and a normalized value very close to the unit (0.83), confirming the active margin distinction for Lemnos Island.
- The relative abundances of Hf and Y, displaying negative anomalies, suggest an active margin tectonic setting. Zr is presented with a positive anomaly reflecting a heavy mineral input that could be considered typical of a passive margin environment. Nevertheless, this positive anomaly according to Bahlburg (1998) is due to reworking and sorting during sediment transfer.
- Relative abundances of Sr and P. The studied sandstones display peaks on the multi-elements diagram, and in association with the presence of Ba and K, with normalized values below unity, the mafic source input for the active margin environment should be considered.

Hence, the REE study suggests an active continental margin character for Lemnos Island. Moreover, processes like reworking and sorting were of great importance during sedimentation, in contrast to processes of intracrustal differentiation, while a mafic source composition is indicated.

PETROGRAPHY AND GEOCHEMISTRY SUBMARINE FANS, LEMNOS ISLAND

Table 4. Summary of the Zr/Th, Y/Ni and Cr/V data for sandstones and mudstones of the late Eocene–early Oligocene Lemnos Island deposits in relation to the value of average upper crust (UCC) of McLennan (2001)

Sample ID	Zr/Th	Y/Ni	Cr/V	Sample ID	Zr/Th	Y/Ni	Cr/V
1 (mudstone)	16.50943	0.109756	1.337931	14 (mudstone)	11.74825	0.25641	1.687898
2 (sandstone)	27.16981	0.207317	3	15 (mudstone)	14.10448	0.188034	1.928571
3 (mudstone)	12.15517	0.193798	1.168605	16 (sandstone)	34.66667	0.211268	4.08
4 (sandstone)	34.61538	0.3125	3.6875	17 (sandstone)	27.87879	0.173333	2.567901
5 (mudstone)	14.24779	0.14557	1.892562	18 (sandstone)	31.30435	0.15625	8.816327
6 (sandstone)	24.13793	0.13913	4.673469	19 (mudstone)	10	0.118056	1.349593
7 (sandstone)	19.52381	0.207921	2.511905	20 (sandstone)	34.09091	0.188889	4.255814
8 (mudstone)	21.64557	0.142857	1.747967	21 (sandstone)	15.8427	0.173228	2.221053
9 (mudstone)	4.303406	1.111111	1.8	22 (sandstone)	68.15385	0.292308	20.07895
10 (sandstone)	36.01852	0.120603	3.341463	23 (sandstone)	18.67925	0.126214	3.632653
11 (mudstone)	10.2381	0.151515	1.296053	24 (mudstone)	9.586777	0.149351	1.20915
12 (sandstone)	29.72603	0.167883	3.166667	25 (sandstone)	35.09434	0.210526	3.5
13 (sandstone)	19.77273	0.134921	2.726316	26 (mudstone)	12.97521	0.175676	1.430657
MEAN	22.85343	0.214016	3.427269	UCC	17.76	0.5	0.78

Table 5. REE abundances of sandstones and mudstones from late Eocene–early Oligocene Lemnos Island deposits

Sample ID	La (ppm)	Ce (ppm)	Nd (ppm)	Sm (ppm)	Eu (ppm)	Tb (ppm)	Yb (ppm)	Lu (ppm)
Sandstones								
2	38.41962	27.16823	15.47117	9.95671	11.49425	< 0.5	6.451613	7.086614
4	44.41417	34.48276	16.87764	10.38961	11.49425	< 0.5	8.870968	9.186352
6	43.05177	30.30303	19.69058	9.090909	8.045977	< 0.5	6.451613	6.56168
7	62.39782	45.97701	29.53586	12.98701	12.64368	< 0.5	9.677419	8.923885
10	68.11989	51.20167	28.1294	14.28571	13.7931	< 0.5	11.69355	11.02362
12	48.77384	37.61755	21.09705	12.12121	12.64368	10.34483	10.8871	10.23622
13	56.67575	43.88715	28.1294	12.12121	12.64368	8.62069	8.467742	8.136483
16	37.60218	28.21317	12.65823	7.792208	8.045977	< 0.5	6.451613	5.774278
17	49.59128	34.48276	21.09705	12.12121	13.7931	< 0.5	10.8871	10.49869
18	32.42507	22.98851	16.87764	7.792208	8.045977	< 0.5	6.048387	6.824147
20	31.60763	25.07837	16.87764	8.658009	9.195402	< 0.5	6.451613	6.036745
21	54.76839	41.79728	22.50352	13.41991	13.7931	< 0.5	8.870968	9.186352
22	43.59673	32.39289	16.87764	9.52381	10.34483	< 0.5	8.467742	8.39895
23	34.33243	27.16823	12.65823	8.658009	8.045977	< 0.5	6.048387	5.774278
25	42.50681	28.21317	15.47117	9.090909	9.195402	< 0.5	7.258065	7.611549
MEAN	45.88556	34.06479	19.59681	10.53391	10.88123		8.198925	8.08399
Mudstones								
1	79.29155	59.56113	35.16174	18.61472	16.09195	< 0.5	12.09677	11.02362
3	111.1717	75.23511	40.78762	19.48052	22.98851	10.34483	12.90323	13.12336
5	71.11717	52.2466	36.56821	14.71861	14.94253	10.34483	10.48387	10.23622
8	56.94823	45.97701	22.50352	12.55411	13.7931	10.34483	8.870968	9.186352
9	85.83106	54.33647	26.72293	9.95671	< 0.5	< 0.5	8.870968	8.923885
11	84.46866	59.56113	32.3488	15.58442	13.7931	< 0.5	9.274194	9.448819
14	96.73025	70.01045	40.78762	18.61472	16.09195	< 0.5	9.677419	9.973753
15	99.18256	72.10031	40.78762	19.91342	18.3908	13.7931	10.08065	9.973753
19	57.76567	47.02194	23.90999	12.12121	11.49425	< 0.5	8.467742	8.661417
24	79.56403	59.56113	33.75527	16.01732	14.94253	< 0.5	10.08065	10.23622
26	83.92371	62.69592	36.56821	16.88312	16.09195	10.34483	11.29032	10.76115
MEAN	82.36314	59.84611	33.62741	15.8599	15.86207		10.19062	10.14078

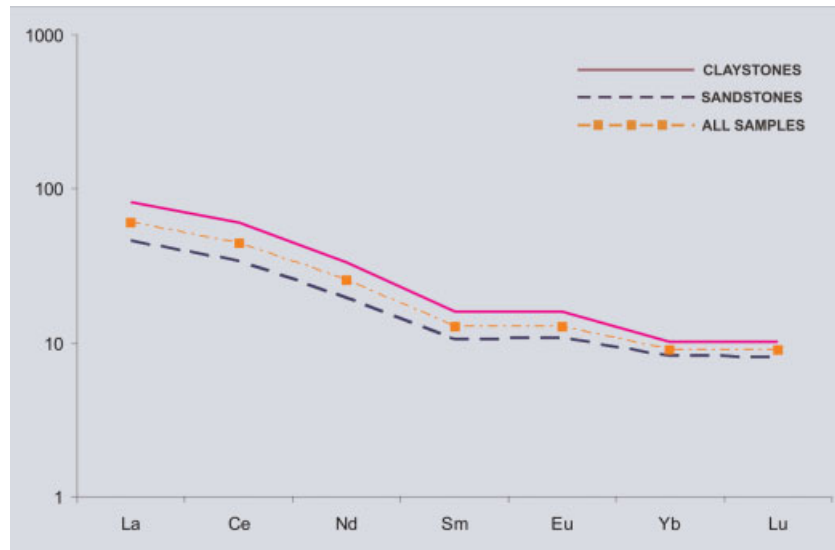


Figure 22. REE pattern of the Lemnos selected samples with REE normalized to chondrite, after Taylor and McLennan (1985).

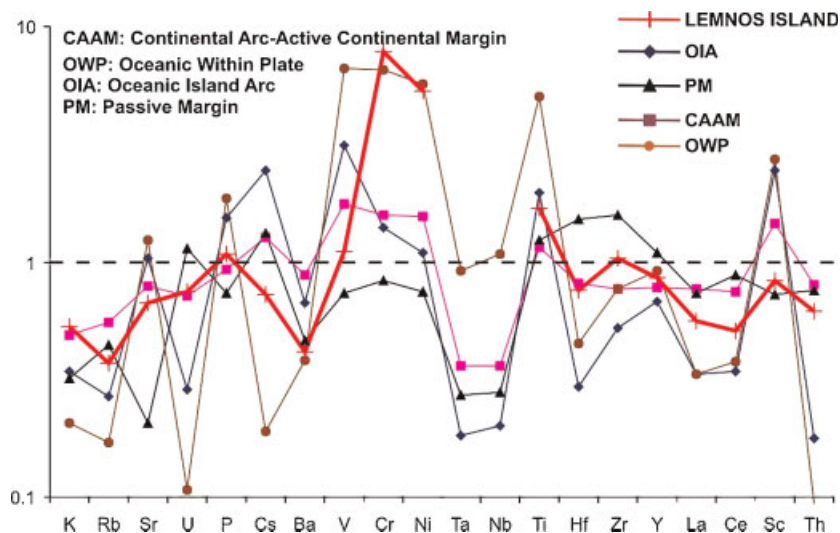


Figure 23. Spider-diagrams with elements standardized on continental crust, after Taylor and McLennan (1985).

6. DISCUSSION

Several geochemical discriminants and diagrams constructed to identify the tectonic setting of sediment deposition (especially sandstones) (e.g. Bhatia 1983; Bhatia and Crook 1986; Roser and Korsch 1986) on the basis of bulk geochemistry contrasts have been applied. The above authors divide sediments into three or four categories (e.g. oceanic island arc, continental island arc, active continental margin and passive margin). Passive margin sediments are those derived from stable continental areas and deposited in plate interiors, Atlantic-type continental margins, failed rifts or grabens or generally along continental margin basins (Bhatia and Crook 1986; Roser and Korsch 1986). Active

margin sediments are deposited at subduction arc margins, strike-slip margins and in proximal positions in backarc basins.

This study attempts to evaluate the provenance and tectonic depositional setting of the selected samples by combining petrography, geochemistry and sedimentology. The application of various discriminant schemes based on major, trace and rare earth elements suggests that the Lemnos sandstones were deposited in an active continental margin environment, where the source area was mostly of mafic/ultramafic composition. Additional data, derived from the modal analysis, suggest origin from igneous, metamorphic and sedimentary source areas, with no or little contribution from magmatic source areas. In addition to the

petrographic characters, NE–NNE palaeocurrent directions, derived from flute and groove marks, collected from the base of the Lemnos sandstones, indicate flow from the southwest, opposite from the locus of the late Eocene–early Oligocene magmatic belt in the Northeast Aegean region (Maravelis *et al.* 2007). This amplifies the mixed igneous, metamorphic and sedimentary provenance signature for the studied sediments. Conglomerates within the study area contain chert, gneiss and igneous fragments, such as basalts and gabbros, suggesting the nature of the source.

Thus, palaeocurrent, geochemical and petrographic data suggest that during late Eocene–early Oligocene (Biozones NP18–Np21b, according to Martini's 1971 classification) Lemnos Island served as a forearc basin of the 'contracted' type (*sensu* Dickinson and Seely 1979). This type of basin bounded on the seaward side by a large accretionary prism, and on the landward flank by a trenchward-dipping backstop of continental crust or island–arc massif (e.g. Lewis and Hayes 1984; Mountney and Westbrook 1997). Hence, the studied area possibly lies between the active volcanic arc, of the Rhodope Zone, and by a structural high, located in the central Aegean Sea (Figure 24). High-precision U–Pb zircon and rutile age dating in the Central Rhodope area (Peytcheva *et al.* 2002), document a southward shift of this magmatism from 92 to 78 Ma. The progressive southward migration of magmatic activity in the Aegean region (Fyticas *et al.* 1984), that commenced in the Rhodope Zone in the Late Eocene (Yanev *et al.* 1998), has been confirmed by seismic tomography (Spakman *et al.* 1988), implying that present-day north-vergent subduction in the Aegean region has started by at least 40 Ma.

The stratigraphic architecture of the sedimentary sequences, within the studied area, characteristically exhibits a successive landward migration of the basin depocentre to the north. According to Lewis and Hayes (1984) and Mountney and Westbrook (1997) this style is possibly due to the fact that the accretionary structural high, bounding the basin's oceanward flank, is forced upward and landward by continued accretion at the toe of the margin.

The study of the Lemnos submarine fan and shelf deposits emphasizes the role of the outer arc ridge (which often serves as a dam to pond sediments in the forearc region) as a major contributor of sediments into the forearc basin. Petrographic and geochemical data suggest that mafic/ultramafic, ophiolite-derived and associated metamorphic rocks and sedimentary carapace served as the main sediment source for the studied deposits. This source delivered ultramafic, gabbro, basalt, chert and possibly, some volcanoclastic detritus of variable size into the adjacent forearc basin (Lemnos Island), and should be located south-southwest of Lemnos Island (Central Aegean region?). The source area could be of rugged topography, where vigorous and erosive processes are common. Such processes caused the ophiolitic bedrock to be incised deeply and rapidly, allowing a significant amount of coarse grained material, from a rapidly uplifting source area, to be made available for sedimentation.

Considering that sediments have an outer arc ridge-arc derivation, an alternative model of possible multiple point sources for the rocks should be considered (Figure 24). This model does not correspond to the studied area, and needs further examination, including the lateral correlation of

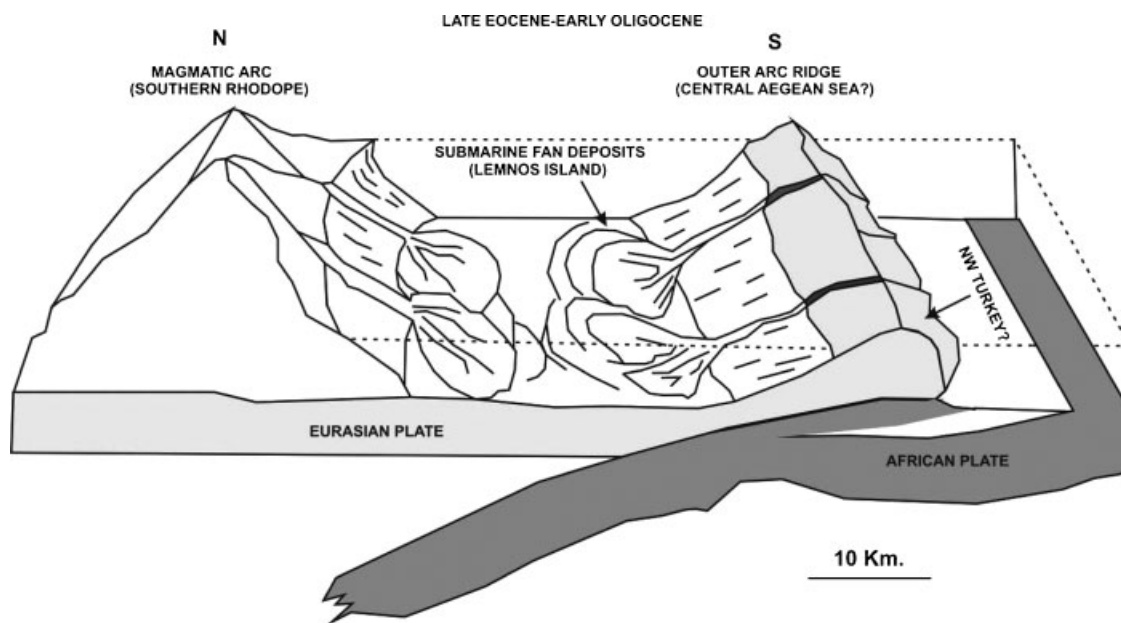


Figure 24. Schematic diagram illustrating the depositional setting of the studied sediments (modified after Queano 2005).

these sediments with age equivalent submarine fan deposits, at the adjacent areas (e.g. NW Turkey).

7. CONCLUSIONS

- Petrographic data from selected samples of sandstones from Lemnos Island demonstrate that they are lithic arenites. The framework grains are mainly quartz but contain also significant amount of feldspar (K-feldspar and plagioclase) and rock fragments (metamorphic, sedimentary and igneous). Petrofacies analysis suggest that metamorphic, sedimentary and plutonic igneous rocks, in a recycled orogenic environment, were the most important source rocks, for the studied sediments. This fact can be related to a subduction complex provenance. The tectonically uplifted subduction complex, composed of ophiolitic and other oceanic material, forms a structural high along the trench–slope break, between the trench axis (Central Aegean?) and the volcanic chain (Rhodope Arc). Sediments, derived from this uplifted structural high, shed north towards the arc, into the forearc basin (Lemnos Island).
- The presence of polycrystalline quartz grains, of both metamorphic and igneous origin, in association with the presence of igneous, metamorphic and sedimentary clasts, within the sandstones, and the limited occurrence of volcanic fragments, suggest a mixed igneous, metamorphic and sedimentary source, with no or little contribution from a magmatic source.
- Major element studies also reveal both, the active continental margin provenance for the Lemnos samples, and the contribution of a mafic/ultramafic source to the studied area. Trace element results suggest an active continental margin or a continental island arc provenance, and a weak degree of recycling for the studied sediments. The minor occurrence of volcanic fragments, within the sandstones, strengthens the argument for an active continental margin tectonic setting. The multi-element diagrams suggest an active margin environment, while the positive anomaly of Zr could be related to reworking and sorting during sediment transfer. Moreover, a mafic/ultramafic source should be considered as the major component, controlling both submarine fans and shelf deposition. The influence of a mafic/ultramafic source is also suggested from the high and variable Cr, Ni and V content, of the intercalations in the distal turbidite facies.
- REE data revealed positive Eu anomalies proposing sedimentary processes, whereby plagioclase is slightly concentrated in the sands because of sorting. This process appears to be related to high normative plagioclase content, due to a local accumulation of feldspar during

sedimentation, suggesting that the process of intra-crustal differentiation (involving plagioclase fractionation) was not of great importance.

The previous conclusions integrated with sedimentological data (e.g. palaeocurrents) suggest that the study area was served as a forearc basin, of the ‘contracted’ type. Palaeomagnetic studies show no rotation of the eastern Rhodope–Thrace region from the Oligocene onwards (Kissel *et al.* 1986; Kissel and Laj 1988). This fact implies that the NE–NNE palaeocurrent direction, recorded in the rocks studied, was the primary direction. Moreover, it emphasizes the role of the outer arc ridge as a major contributor of sediments into the forearc basin. Both, petrographic and geochemical data suggest that mafic/ultramafic, ophiolite-derived and associated metamorphic rocks and the sedimentary carapace, served as the main sediment source for the studied deposits. This source delivered ultramafic, gabbro, basalt, chert and, possibly, some volcanoclastic detritus, of variable size, into the adjacent forearc basin (Lemnos Island), and should be searched south-southwest from Lemnos Island (Central Aegean region?).

ACKNOWLEDGEMENTS

This research project (PENED) is co-financed by E.U.-European Social Fund (80%) and the Greek Ministry of Development-GSRT (20%). The authors would like to thank the chief editor Professor Ian Somerville, the editor Dr Alistair Ruffell and the two reviewers for their constructive comments which improved the paper. The authors also gratefully acknowledged Dr Jose Arribas for his helpful comments on an earlier draft of the manuscript.

REFERENCES

- Abdel-Wahab AA. 1992.** Provenance of Gebel El-Zeit sandstones, Gulf of Suez, Egypt. *Sedimentary Geology* **75**: 241–255.
- Aldanmaz E, Pearce JA, Thirlwall MF, Mitchel JG. 2000.** Petrogenetic evolution of late Cenozoic, post-collision volcanism in western Anatolia, Turkey. *Journal of Volcanology and Geothermal Research* **102**: 67–95.
- Angelier J, Lyberis N, Le Pichon X, Barrier E, Huchon P. 1982.** The tectonic development of the Hellenic arc and the Sea of Crete, a synthesis. *Tectonophysics* **86**: 159–196.
- Armijo R, Meyer B, Hubert A, Barka A. 1999.** Westward propagation of the North Anatolian Fault into the northern Aegean: timing and kinematics. *Geology* **27**: 267–270.
- Armstrong-Altrin JS, Lee Y, Verma S, Ramasamy S. 2004.** Geochemistry of sandstones from the Upper Miocene Kudanul Formation, southern India: implications for provenance, weathering and tectonic setting. *Journal of Sedimentary Research* **74**(2): 167–179.
- Arribas J, Cristelli S, Le Pera E, Tortosa A. 2000.** Composition of modern stream sand derived from a mixture of sedimentary and meta-

- morphic source rocks (Henares River Central Spain). *Sedimentary Geology* **133**(1–4): 27–48.
- Asiedu DK, Suzui S, Shibata T. 2000.** Provenance of sandstones from the Lower Cretaceous Sasayama Group, inner zone of southwest Japan. *Sedimentary Geology* **131**: 9–24.
- Bahlburg H. 1998.** The geochemistry and provenance of Ordovician turbidites in the Argentine Puna. In *The Proto-Andean Margin of Gondwana*, Pankhurst RJ, Rapela CW (eds). Geological Society of London, Special Publications, Bath, UK **142**: 127–142.
- Basu A, Young S, Suttner L, James W, Mack G. 1975.** Re-evaluation of the use of undulatory extinction and crystallinity in detrital quartz for provenance interpretation. *Journal of Sedimentary Petrology* **45**: 873–882.
- Bhatia MR. 1983.** Plate tectonics and geochemical composition of sandstones. *Journal of Geology* **91**(6): 611–627.
- Bhatia MR. 1985.** Rare-earth element geochemistry of Australian Paleozoic greywackes and mudrocks: provenance and tectonic control. *Sedimentary Geology* **45**: 97–113.
- Bhatia MR, Crook KAW. 1986.** Trace elements characteristics of graywackes and tectonic setting discrimination of sedimentary basins. *Contributions to Mineralogy and Petrology* **92**: 181–193.
- Blatt H, Middleton G, Murray R. 1980.** *Origin of Sedimentary Rocks*. 2nd edn Prentice-Hall: Englewood Cliffs, NJ.
- Bock B, McLennan SM, Hanson GN. 1994.** Rare earth element redistribution and its effects on the neodymium isotope system in the Austin Glen Member of the Normanskill Formation, New York, USA. *Geochimica et Cosmochimica Acta* **58**: 5245–5253.
- Bock B, Bahlburg H, Wörner G, Zimmermann U. 2000.** Ordovician arcs and terranes in NW-Argentina and N-Chile. Geochemical and isotope evidence. *Journal of Geology* **108**: 513–535.
- Bonchev E. 1980.** The Transbalkan strip of post-Lutetian tectonomagmatic and metallogenic mobilisation. *Geologica Balcanica* **10**(4): 3–34.
- Bonin B, Brandlein P, Bussy F, Desmons J, Eggenberger U, Finger F, Graf K, Vivier G. 1993.** Late Variscan magmatic evolution of the Alpine basement. In *Pre-Mesozoic Geology in the Alps*, Springer, Verlag, Berlin: 171–202.
- Burnett DJ, Quirk DG. 2001.** Turbidite provenance in the Lower Paleozoic Manx Group, Isle of Man: implications for the tectonic setting of Eastern Avalonia. *Journal of Geological Society of London* **158**: 913–924.
- Crook KAW. 1974.** Lithogenesis and geotectonics: the significance of compositional variations in flysch arenites (graywackes). In *Modern and Ancient Geosynclinal Sedimentation*, Dott Jr, Shaver RH (eds). SEPM Special Publications, Tulsa, Oklahoma, USA **19**: 304–310.
- Cvetkovic V, Harkovska A, Karamata S, Knezevic V, Memovic E, Pecskey Z. 1995.** Correlation of some Oligocene volcanic complexes along the west–east traverse in Central Balkan Peninsula. *Proceedings of the XV Congress CBGA*, 1995, Athens, Greece, 501–505.
- Dabovski C. 1991.** Modern concepts on the evolution of the Alpine orogen in the Eastern Mediterranean and Carpathian–Balkan area. A review and some problems of Bulgarian geotectonics. *Geotectonic Tectonophysics and Geodynamic* **22**: 45–79.
- Dickinson WR. 1985.** Interpreting provenance relations from detrital modes of sandstones. In *Provenance of Arenites*, Zuffa GG (ed.). Reide, Dordrecht, Boston, USA: 333–336.
- Dickinson WR, Seely DR. 1979.** Structure and stratigraphy of forearc regions. *The American Association of Petroleum Geologists Bulletin* **63**: 2–31.
- Dickinson WR, Suczek C. 1979.** Plate tectonics and sandstone composition. *American Association of Petroleum Geologists Bulletin* **63**: 2164–2182.
- Dickinson WR, Beard LS, Brakenridge GR, Erjavec JL, Ferguson RC, Inman KF, Knepp RA, Lindberg FA, Ryberg PT. 1983.** Provenance of North American Phanerozoic sandstones in relation to tectonic setting. *Geological Society of America Bulletin* **94**: 222–235.
- Dinter D. 1994.** Tertiary structural evolution of the southern Rhodope metamorphic province: a fundamental revision. *Bulletin of the Geological Society of Greece* **30**(1): 79–89.
- Dinter DA, Royden L. 1993.** Late Cenozoic extension in northeastern Greece: Strymon valley detachment and Rhodope metamorphic core complex. *Geology* **21**: 45–48.
- Dinter D, Macfarlane A, Hames W, Isachsen C, Bowring S, Royden L. 1995.** U–Pb and Ar/Ar geochronology of the Symvolon granodiorite: implications for the thermal and structural evolution of the Rhodope metamorphic core complex, northeastern Greece. *Tectonics* **14**: 886–908.
- Feng R, Kerrich R. 1990.** Geochemistry of fine-grained clastic sediments in the Archean Abitibi greenstone belt, Canada: implications for provenance and tectonic setting. *Geochimica et Cosmochimica Acta* **54**: 1061–1081.
- Floyd PA, Leveridge BE. 1987.** Tectonic environment of the Devonian Gramscatho basin, south Cornwall: framework mode and geochemical evidence from turbidite sandstones. *Journal of the Geological Society of London* **144**: 531–542.
- Floyd PA, Shail R, Leveridge BE, Franke W. 1991.** Geochemistry and provenance of Rhenoherynian synorogenic sandstones: implications for tectonic environment discrimination. In *Developments in Sedimentary Provenance Studies*, Morton AC, Todd SP, Haughton PDW (eds). Geological Society of America Special Publications, Bath, UK **57**: 611–626.
- Folk RL. 1974.** *Petrology of Sedimentary Rocks*, 2nd edn Hemphill Press: Austin, TX.
- Fyticas M, Innocenti F, Manetti P, Mazzuoli R, Peccerillo A, Villari L. 1984.** Tertiary to Quaternary evolution of the volcanism in the Aegean Region. In *The Geological Evolution of the Eastern Mediterranean*, Dixon JE, Robertson AHF (eds). Geological Society of London, Special Publications, Bath, UK **17**: 687–699.
- Gu XX. 1994.** Geochemical characteristics of the Triassic Tethys-turbidites in the northwestern Sichuan, China: implications for provenance and interpretation of the tectonic setting. *Geochimica et Cosmochimica Acta* **58**: 4615–4631.
- Harkovska A, Yanev Y, Marchev P. 1989.** General features of the Paleogene orogenic magmatism in Bulgaria. *Geologica Balcanica* **19**(1): 37–72.
- Hoffman EL. 1992.** Instrumental neutron activation in geoanalysis. *Journal of Geochemical Exploration* **44**: 297–319.
- Ingersoll RV, Suczek CA. 1979.** Petrology and provenance of Neogene sand from Nicobar and Bengal fans, DSDP sites 211 and 218. *Journal of Sedimentary Petrology* **49**: 1217–1228.
- Ingersoll RV, Bullard T, Ford R, Grimm J, Pickle J, Sares S. 1984.** The effect of grain size on detrital modes: a test of the Gazzi Dickinson point-counting method. *Journal of Sedimentary Petrology* **54**: 103–116.
- Jolivet L, Brun JP, Gautier P, Lallemand S, Patriat M. 1994.** 3D kinematics of extension in the Aegean region from the early Miocene to the present, insights from the ductile crust. *Bulletin of the Geological Society of France* **165**: 195–209.
- Kissel C, Laj C. 1988.** The tertiary geodynamical evolution of the Aegean arc: a paleomagnetic reconstruction. *Tectonophysics* **146**: 183–201.
- Kissel C, Kondopoulou D, Laj C, Papadopoulos P. 1986.** New paleomagnetic data from Oligocene formations of Northern Aegean. *Geophysical Research Letters* **13**: 1039–1042.
- Kroonenberg SB. 1994.** Effects of provenance, sorting and weathering on the geochemistry of fluvial sands from different tectonic and climatic environments. *Proceedings of the 29th International Geological Congress*, Part A, 69–81.
- Kuttelolf S, Diener R, Schacht U, Krawinkel H. 2007.** Provenance of the Carboniferous Hochwipfel Formation (Karawanken Mountains, Austria/Slovenia) Geochemistry versus petrography. *Sedimentary Geology* **203**: 246–266.
- Le Pichon X, Angelier J. 1979.** The Aegean arc and trench system: a key to the neotectonic evolution of the Eastern Mediterranean area. *Tectonophysics* **60**: 1–42.
- Lewis S, Hayes DE. 1984.** A geophysical study of the Manila Trench, Luzon, Philippines. 2. Fore-arc basin structural and stratigraphic evolution. *Journal of Geophysical Research* **89**: 9196–9214.
- Maravelis A, Konstantopoulos P, Pantopoulos G, Zeliidis A. 2007.** North Aegean sedimentary basin evolution during the late Eocene to early Oligocene based on sedimentological studies on Lemnos Island (NE Greece). *Geologica Carpathica* **58**: 455–464.

- Marchev P, Shanov S. 1991.** Potassium and silica variations in the Paleogene Macedonian–Rhodope–North Aegean Volcanic Belt: geodynamic and petrogenetic implications. *Geologica Balcanica* **21**(2): 3–11.
- Martini E. 1971.** Standard Tertiary and Quaternary calcareous nannoplankton zonation. *2nd International Conference on Planktonic Microfossils*, Roma **2**, 739–785.
- Maynard JB, Valloni R, Yu H. 1982.** Composition of modern deep sea sands from arc-related basins. *Geological Society of London, Special Publication* **10**: 551–561.
- McCann T. 1991.** Petrological and geochemical determination of provenance in the southern Welsh Basin. In *Developments in Sedimentary Provenance Studies*, Morton AC, Todd SP, Haughton PDW (eds). Geological Society of America Special Publications, Bath, UK **57**: 215–230.
- McDaniel DK, Hemming SR, McLennan SM, Hanson GN. 1994.** Resetting of neodymium isotopes and redistribution of REEs during sedimentary processes. The Early Proterozoic Chelmsford Formation, Sudbury Basin, Ontario, Canada. *Geochimica et Cosmochimica Acta* **58**: 931–941.
- McKenzie DP. 1970.** Plate tectonics of the Mediterranean region. *Nature* **226**: 239–243.
- McKenzie DP. 1978.** Some remarks on the development of sedimentary basins. *Earth and Planetary Science Letters* **40**: 25–32.
- McLennan SM. 1989.** Rare earth elements in sedimentary rocks: influence of provenance and sedimentary process. In *Geochemistry and Mineralogy of Rare Earth Elements*, Lipin BR, McKay GA (eds). Mineralogical Society of America, Washington, (Reviews in mineralogy) **21**: 169–200.
- McLennan SM. 2001.** Relationships between the trace element composition of sedimentary rocks and upper continental crust. *Geochemistry Geophysics Geosystems* **2**(4): 1021.
- McLennan SM, Taylor SR, Eriksson KA. 1983.** Geochemistry of Archean shales from the Pilbara Supergroup, Western Australia. *Geochimica et Cosmochimica Acta* **47**: 1211–1222.
- McLennan SM, Taylor SR, McCulloch MT, Maynard JB. 1990.** Geochemical and Nd–Sr isotopic composition of deep-sea turbidites: crustal evolution and plate tectonic associations. *Geochimica et Cosmochimica Acta* **54**: 2015–2050.
- McLennan SM, Hemming S, McDaniel DK, Hanson GN. 1993.** Geochemical approaches to sedimentation, provenance and tectonics. In *Processes Controlling the Composition of Clastic Sediments*, Johnson MJ, Basu A (eds). Geological Society of America Special Paper, Boulder, Colorado **284**: 21–40.
- Meulenkamp JE, Wortel MJR, Van Wamel WA, Spakman W, Hoogerduyn E. 1988.** Strating, on the Hellenic subduction zone and the geodynamic evolution of Crete since the late Middle Miocene. *Tectonophysics* **146**: 203–215.
- Milodowski AE, Zalasiewicz JA. 1991.** Redistribution of rare earth elements during diagenesis of turbidite/hemipelagite mudrock sequences of Llandovery age from Central Wales. In *Developments in Sedimentary Provenance Studies*, Morton AC, Todd SP, Haughton PDW (eds). Geological Society of America Special Publications, Bath, UK **57**: 101–124.
- Morton AC. 1985.** Heavy minerals in provenance studies. In *Provenance of Arenites*, Zuffa GG (ed.). NATOASI Series No **148**, D. Reidel Pub. Co, Dordrecht, Boston, USA, 249–277.
- Morton AC, Davies JR, Waters RA. 1992.** Heavy minerals as a guide to turbidite provenance in the Lower Palaeozoic Southern Welsh Basin: a pilot study. *Geological Magazine* **129**: 573–580.
- Mountney NP, Westbrook GK. 1997.** Quantitative analysis of Miocene to Recent forearc basin evolution along the Columbian convergent margin. *Basin Research* **9**: 177–196.
- Nance WB, Taylor SR. 1977.** Rare earth element patterns and crustal evolution II: Archean sedimentary rocks from Kalgoorlie, Australia. *Geochimica et Cosmochimica Acta* **41**: 225–231.
- Papazachos BC, Papadimitriou EE, Kiratzi AA, Papazachos CB, Louvari EK. 1998.** Fault plane solutions in the Aegean Sea and the surrounding area and their tectonic implication. *IASPEI, 29th General Assembly, Abstracts*, 17.
- Pe-Piper G, Piper DJW. 2001.** Late Cenozoic, post-collisional Aegean igneous rocks: Nd, Pb and Sr isotopic constraints on petrogenetic and tectonic models. *Geological Magazine* **138**: 653–668.
- Pettijohn FJ, Potter PE, Siever R. 1973.** *Sand and Sandstone*. Springer: Verlag, Berlin; 553.
- Pettijohn FJ, Potter PE, Siever R. 1987.** *Sand and Sandstone*, 2nd edn Springer: New York; 553.
- Peytcheva I, Von Quadt A, Heinrich C, Ivanov Z, Kamenov B, Kouzmanov K. 2002.** Evolution of magmatism and related ore formation in Central Srednogie, Bulgaria: new insight from high-precision U–Pb zircon and rutile geochronology and isotope tracing. GEODE Study Center on Geodynamics and ore deposit evolution. Chateau de Passieres, near Grenoble 25–28 October 2002.
- Queano LK. 2005.** Upper Miocene to Lower Pliocene Sigaboy formation turbidites, on the Pujada Peninsula, Mindanao, Philippines: internal structures, composition, depositional elements and reservoir characteristics. *Journal of Asian Earth Science* **25**: 387–402.
- Roser BP, Korsch RJ. 1986.** Determination of tectonic setting of sandstone–mudstone suites using SiO₂ and K₂O/Na₂O ratio. *Journal of Geology* **94**: 635–650.
- Roser BP, Korsch RJ. 1988.** Provenance signatures of Sandstone–Mudstone suites determined using discriminant function analysis of major-element data. *Chemical Geology* **67**: 119–139.
- Roser BP, Cooper RA, Nathan S, Tulloch AJ. 1996.** Reconnaissance sandstone geochemistry, provenance, and tectonic setting of the lower Paleozoic terranes of the West Coast and Nelson, New Zealand. *New Zealand Journal of Geology and Geophysics* **39**: 1–16.
- Shaw DM. 1968.** A review of K–Rb fractionation trends by covariance analysis. *Geochimica et Cosmochimica Acta* **32**: 573–602.
- Spakman W, Wortel MJR, Vlaar NJ. 1988.** The Hellenic subduction zone: a tomographic image and its geodynamic implications. *Geophysical Research Letters* **15**: 60–63.
- Taylor SR, McLennan SM. 1985.** *The Continental Crust: Its Composition and Evolution*. Blackwell Scientific: Oxford; 312.
- Tortosa A, Palomares M, Arribas J. 1991.** Quartz grain types in Holocene deposits from the Spanish central system: some problems in provenance analysis. In *Developments in Sedimentary Provenance Studies*, Morton AC, Todd SP, Haughton PDW (eds). Geological Society of America Special Publications, Bath, UK **57**: 47–454.
- Utzmann A, Hansteen TH, Schmincke HU. 2002.** Trace element mobility during sub-seafloor alteration of basaltic glass from Ocean Drilling Program site 953 (off Gran Canaria). *International Journal of Earth Sciences* **91**: 661–679.
- Wanas HA, Abdel-Maguid NM. 2006.** Petrography and geochemistry of the Cambro-Ordovician Wajid Sandstone, southwest Saudi Arabia: implications for provenance and tectonic setting. *Journal of Asian Earth Sciences* **27**: 416–429.
- Yanev Y, Stoykov S, Pecskey Z. 1998.** Petrology and K–Ar dating of the Paleogene magmatism in the region of the villages Yabalkovo and Stalevo, Eastern Rhodopes volcanic area. *Mineralogy Petrology Geochemistry* **34**: 97–110. (In Bulgarian with English abstract).
- Yilmaz Y, Polat A. 1998.** Geology and evolution of the Thrace volcanism, Turkey. In *Tertiary Magmatism of the Rhodopian Region*, Christofides G, Marchev P, Serri G (eds). Acta Vulcanologica, Pisa–Roma **10**(2): 293–304.
- Young SW. 1976.** Petrographic textures of detrital polycrystalline quartz as an aid to interpreting crystalline source rocks. *Journal of Sedimentary Petrology* **46**: 595–603.
- Zhao JX, McCulloch MT, Bennett VC. 1992.** Sm–Nd and U–Pb zircon isotope constraints on the provenance of sediments from the Amadeus Basin, central Australia: evidence for REE fractionation. *Geochimica et Cosmochimica Acta* **56**: 921–940.
- Zimmermann U, Bahlburg H. 2003.** Provenance analysis and tectonic setting of the Ordovician clastic deposits in the southern Puna Basin, NW Argentina. *Sedimentology* **50**: 1079–1104.
- Zuffa GG. 1985.** Optical analyses of arenites: influence of methodology on compositional results. In *Provenance of Arenites*, Zuffa GG (ed.). NATOASI Series No **148**, D. Reidel Pub. Co, Dordrecht, Boston, USA: 165–189.